GIN, ALLEN WILLIAM

THE STUDY OF COMPLEXES OF HETEROCYCLIC BASES BY UV PHOTOELECTRON SPECTROSCOPY

City University of New York PH.D. 1980

THE STUDY OF COMPLEXES OF HETEROCYCLIC BASES BY UV PHOTOELECTRON SPECTROSCOPY

by

ALLEN GIN

A dissertation submitted to the Graduate Faculty in Chemistry in partial fulfillment of the requirements for the degree of Doctor of Philosophy, The City University of New York.

1980

This manuscript has been read and accepted for the Graduate Faculty in Chemistry in satisfaction of the dissertation requirement for the degree of Doctor of Philosophy.

7/24/80
date

Chairman of Examining Committee

24 July 1980
date

David C. Lorden
Executive Officer

Michael A. Weiner

Thomas Halgren

Arthur D. Baker
Supervisory Committee

The City University of New York

ACKNOWLEDGEMENTS

I wish to express my sincere appreciation to Professor Michael Weiner for his guidance over my thesis research. It was he who first suggested the research ideas, and the results of this thesis are a culmination of these ideas, as well as our numerous discussions. His expert knowledge, amiability, and extreme helpfulness made my learning experience all the more rewarding.

I wish to thank Professor Arthur Baker for sharing his valuable knowledge of the Photoelectron Spectrometer with me, and Professor Thomas Halgren, for his suggestions in regard to the computational aspects. In addition, I want to express my gratitude to Professor Jay Kochi, of the University of Indiana, for supplying the tin complexes.

Finally, I would like to express my appreciation to my parents and K. Bunding for their support throughout my career as a graduate student. It is to them that this work is dedicated.

TABLE OF CONTENTS

LIST OF TABLES

LIST OF FIGURES

THE STUDY OF COMPLEXES OF HETEROCYCLIC BASES BY UV PHOTOELECTRON SPECTROSCOPY

by

ALLEN GIN

ABSTRACT

The UV photoelectron spectra of $Cr(CO)_5 \cdot L$, $BH_3 \cdot L$ and $BF_3 \cdot L$ (where L = 4-substituted pyridine) were measured, and the ionization potentials observed below 12 eV are discussed. For $Cr(CO)_5 \cdot L$, bands found in the region 7-8 eV are assigned to ionization from the d-orbitals. The IP values increase with the increasing electron acceptor nature of the ring substituents. The remaining bands below 12 eV are assigned to the pyridine orbitals. The IP values of the uncomplexed pyridine increase on complexation, and a comparison is made of the effects of complexation with the $CR(CO)_5$ and BH_3 moieties. MNDO calculations were utilized to explain the increases in $a_2(\pi)$ and $b_1(\pi)$ energies upon borane and boron trifluoride complexation. The increase

in $a_2(\pi)$ upon adduct formation can be related to changes in charge densities. Symmetry conditions prevent orbital interactions between the $a_2(\pi)$ and π components of the acid or substituent. Since the $b_1(\pi)$ orbital can be perturbed by orbital interactions, a simple explanation for the energy changes of $b_1(\pi)$ upon complexation is not possible.

The ionization potentials of symmetric and unsymmetric tetraalkyltin compounds (R_4Sn, $RSnMe_3$ and R_2SnMe_2; R = alkyl groups) are correlated linearly with the sum of the Taft σ^* values ($\Sigma\sigma^*$) for the alkyl ligands only if the weighted average $\overline{IP}$ values are used. This takes into account the orbital degeneracy of the lowest energy bands in the photoelectron spectra.

PART I

GENERAL INTRODUCTION

General Introduction

Ultraviolet photoelectron spectroscopy (pes) was developed in the early 1960's independently by two groups, one led by Turner[1,2] in London, and the other by Vilesov[3] in Leningrad. It was Turner's design of the He(I) radiation source that led to the development of a commercial photoelectron spectrometer by Perkin-Elmer in the early 1970's. Subsequently, many thousands of papers, review articles[4a,b,c] and books[5a,b,c,d] have found their way into the scientific literature.

Photoelectron spectroscopy is an extremely useful probe in elucidating the electronic structure of atoms and molecules. Monoenergetic photons of energy $h\nu$ interact with molecules that have electrons bound by energy E_j, resulting in ejection of electrons with kinetic energy KE_j. Conservation of energy between the cation and electron requires that

$$KE = h\nu - E_j \qquad (1)$$

where E_j is the ionization energy or potential of the electron in the molecule. This is an application of Einstein's photoelectric law.

An adiabatic ionization potential (IP_a) is defined as the minimum energy required to eject an electron from a molecule in its ground electronic and vibrational state, and transform it into a positive ion in the lowest vibrational level. This is often not realized because the potential surfaces of the states involved are not vertical. A non-adiabatic transition (IP_v) has the same geometry in the excited ionic state as the ground state. An ionization of this type is defined as a vertical ionization (IP_v). This is the band maximum in a photoelectron ionization band. For a non-bonding or weakly bonding electron, $IP_v = IP_a$. For a bonding electron, $IP_v > IP_a$.

Koopmans' theorem states that the molecular ionization energies are equal to the negatives of the molecular orbital eigenvalues.[6]

$$IP_{v,j} = -\varepsilon_j \qquad (2)$$

Although the theorem makes substantial assumptions it has been extremely successful in interpreting photoelectron spectra.

In the present study, pes data were collected on a Perkin-Elmer Model PS-18 Photoelectron Spectrometer. The He(I) source generates monoenergetic radiation at

21.21 eV (over 98% pure) from a 2 KV DC Helium discharge. The detectors used were either the electron multiplier (EMI type 9643/2B) or the channel multiplier (Mullard B 419 BL). Spectra were calibrated with argon ($^2P_{3/2}$, 15.759 eV line) and xenon ($^2P_{3/2}$, 12.130 eV line), used as internal calibrants. Sometimes methyl iodide ($^2E_{3/2}$, 9.538 eV line) was used to calibrate a larger range. The working resolution was usually about 20 MeV (full width at half height of $^2P_{3/2}$) for the 15.759 eV argon line. This diminished to 50 MeV at times. Pressure in the main chamber was below $2x10^{-5}$ torr. Ionization energies were read as vertical IP's (peak maxima) unless otherwise noted. A direct inlet probe was used for samples which required elevated temperatures, while a volatile probe was used for samples with adequate vapor pressure at ambient temperature (see Table 1).

Table 1: Temperature Ranges Necessary to Obtain Photoelectron Spectra

Compound	Temperature Range (^{o}C)
R_4Sn	volatile probe
$Cr(CO)_5 \cdot$ 4-RPyridine	60-115^{o}
$BF_3 \cdot$ 4-RPyridine	80-150^{o}
$BH_3 \cdot$ 4-RPyridine	45-120^{o}
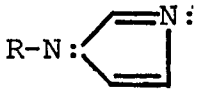	volatile probe
4-RPyridine	volatile probe
	90-115^{o}

PART II

UV PES STUDY OF $Cr(CO)_5$PYRIDINES

Background

Lloyd and Hillier[7] have reported the pes of some $M(CO)_5L$ complexes, where M = Cr or W and L = amine or phosphine (see Table 2). These complexes have local symmetry C_{4v} about the central atom. In this environment a splitting of the t_{2g} orbitals of unsubstituted $M(CO)_6$ (largely on the metal) into b_2 and e components is expected. Lloyd and Hillier observed a destabilization as well as a splitting of the d orbitals. The magnitude of splitting depended on the donor L; ca. 0.30 eV for the ligands with nitrogen, and ca. 0.15 eV for ligands with phosphorus. Intensity considerations suggest that the ^2E ionic state is higher in energy than the $^2B_2$ state, whereas ab initio self-consistent field MO calculations (SCF-MO) of $Cr(CO)_5NH_3$ and $Cr(CO)_5PH_3$ indicate that the e set of orbitals is more stable than b_2 by 0.08 eV and 0.19 eV, respectively (see Table 3). Thus, the pes observation is not apparently consistent with calculations. However, Lloyd and Hillier estimated that the e orbitals should have an 0.5 eV greater relaxation energy than the b_2 orbital, and this could explain the reversed ordering of ionic states from the calculated ground states. This relaxation energy is a consequence of the electron rearrangement (orbital rescaling) of the

Table 2: Vertical Ionization Potentials (eV) of $M(CO)_5L$ Complexes[a]

Complex	IP_1[b]	IP_2[c]	IP_3[d]
$Cr(CO)_6$	8.40(t_{2g})		
$Cr(CO)_5NH_3$	7.56	7.85	
$Cr(CO)_5NMe_3$	7.45	7.76	10.57
$Cr(CO)_5PH_3$	7.90sh	8.03	11.43
$Cr(CO)_5PMe_3$	7.58sh	7.72	10.00
$Cr(CO)_5CNMe$	7.61sh	7.77	
$Cr(CO)_5NH(CH_2)_5$[e]	7.39	7.69	10.50
$W(CO)_6$	8.56(t_{2g})		
$W(CO)_5NH_3$	7.63	7.74	
$W(CO)_5NHMe_2$	7.50	7.74	11.14
$W(CO)_5NMe_3$	7.50	7.74	10.75
$W(CO)_5NH(CH_2)_5$	7.42	7.68	10.59

[a]Ref. 7. [b]IP_1 is assigned to the e set of the metal. For tungsten complexes the spin-orbit coupling has been adjusted. [c]IP_2 is assigned to the b_2 orbital of the metal. For the tungsten complexes the spin-orbit coupling has been adjusted. [d]IP_3 has been assigned to the metal-ligand bonding pair. [e]Ref. 8.

Table 3: Summary of **Ab Initio** Calculations of $Cr(CO)_5NH_3$ and $Cr(CO)_5PH_3$[a]

Koopmans' theorem IP/eV	$Cr(CO)_6$	$Cr(CO)_5NH_3$	$Cr(CO)_5PH_3$
	$10.7(t_{2g})$	$9.25(b_2)$	$9.50(b_2)$
		$9.33(e)$	$9.69(e)$
		$14.8\ (a_1)$	$12.0\ (a_1)$
Orbital character (%)	Cr(3d)75	Cr(3d)67	Cr(3d)71
	C(2p) 8	C(2p)12 b_2	C(2p)10 b_2
	O(2p)17	O(2p)19	O(2p)18
		Cr(3d)78	Cr(3d)79
		C(2p) 7 e	C(2p) 7 e
		O(2p)18	O(2p)14
Atomic charges Cr	+0.70	+0.71	+0.67
C	+0.23	+0.21	+0.22
O	-0.35	-0.37	-0.37
N,P		-0.72	-0.18

[a]Reference 7

cation. Moreover, the calculations show the e orbitals have greater metal character than the b_2 orbital, consistent with a larger relaxation energy.[7] Thus, it seems that as a result of a deviation from Koopmans' theorem, determination of absolute and even relative metal d orbital energies from IP values is imprudent.

H. Daaman and A. Oskam[8] have measured the electronic spectra of $Cr(CO)_5$:4-RPyridine in isoctane (see Table 4). There are two metal to metal transitions; the more intense lower energy band is attributed to $d(e) \rightarrow d(\pi^*)$ and the less intense higher energy band to $d(b_2) \rightarrow d(\pi^*)$. This suggests that the e set is higher in energy than the b_2 orbital in contradiction to the ab initio calculations of Lloyd and Hillier, but in agreement with pes results.

In most of the pes of $Cr(CO)_5L$, a clearly resolved ionization due to the $a_1(\sigma_{M-L})$ orbital is also observed (see Table 2). In the case of PMe_3 and NMe_3 derivatives, the IP's of the donor orbitals are stabilized by 1.37 eV and 2.08 eV respectively from the lone pair (a_1) energies of the uncomplexed ligands.[8] This appears to indicate that the amine is more tightly bound to the chromium, consistent with the calculations on the phosphine and amine complexes.[7]

Table 4: Electronic Transitions of $Cr(CO)_5$ L in Iso-octane (kK)[a]

L	d → d[b]	d → d[c]	d → π*(L)[d]
pyridine	25.7	29.8	25.7
4-picoline	23.9	30.5	26.9
2-picoline	24.8	30.1	27.3
4-t-butylpyridine	24.0	30.0	26.8
2,4-lutidine	23.9	30.5	27.5
4-Clpyridine	24.8	29.9	24.8
4-Brpyridine	24.8	29.4	24.8
pyrazine	24.8	----	21.6
pyridazine	24.2	----	21.8
piperidine[e]	24.0	----	----

[a]Reference 8. [b]First ligand field band was assigned to the $E \rightarrow {}^1A_1$ transition from d_{xz}, d_{yz} to the anti-bonding d_{z^2}. [c]Second ligand field transition with lower intensity. [d]Charge-transfer band is most intense. [e]Benzene solution.

The pes of $M(CO)_5$amine complexes[8] revealed that there was no simple relationship between the ligand pK_a values, the lone pair ionization potentials in the free ligands, and the stabilization energies upon complexation. For example, the lone pair stabilization energy upon complexation for $Cr(CO)_5NMe_3$ is 2.12 eV, and for $Cr(CO)_5$piperidine it is 1.83 eV, despite the fact that piperidine has a larger pK_a value than trimethylamine. Moreover, the pK_a value of piperidine is higher than dimethylamine, but the order of lone pair ionization energies are reversed. However, B. Ramsey and F. Walker[9] did show a linear relationship between substituted pyridine lone pair IP_v's and their solution pK_a values. Figure 1 shows a plot of pK_a vs. IP_v for 17 substituted pyridines, such that $pK_a = -6.80IP(eV) + 70.7$, with an average deviation of $\pm .2$ pK_a units.

M. Weiner and M. Lattman[10] have reported the pes of some $Cr(CO)_5L$ complexes containing various organosulfide and organophosphine ligands (see Table 5). They observed a splitting of the ionization from the d orbitals (IP_1, IP_2) resulting from a breakdown of the degeneracy of the filled t_{2g} orbitals into e and b_2 components. However, they could not assign the two IP's on the basis of intensity considerations in the manner that Lloyd had done for $Cr(CO)_5$amine. They identified the

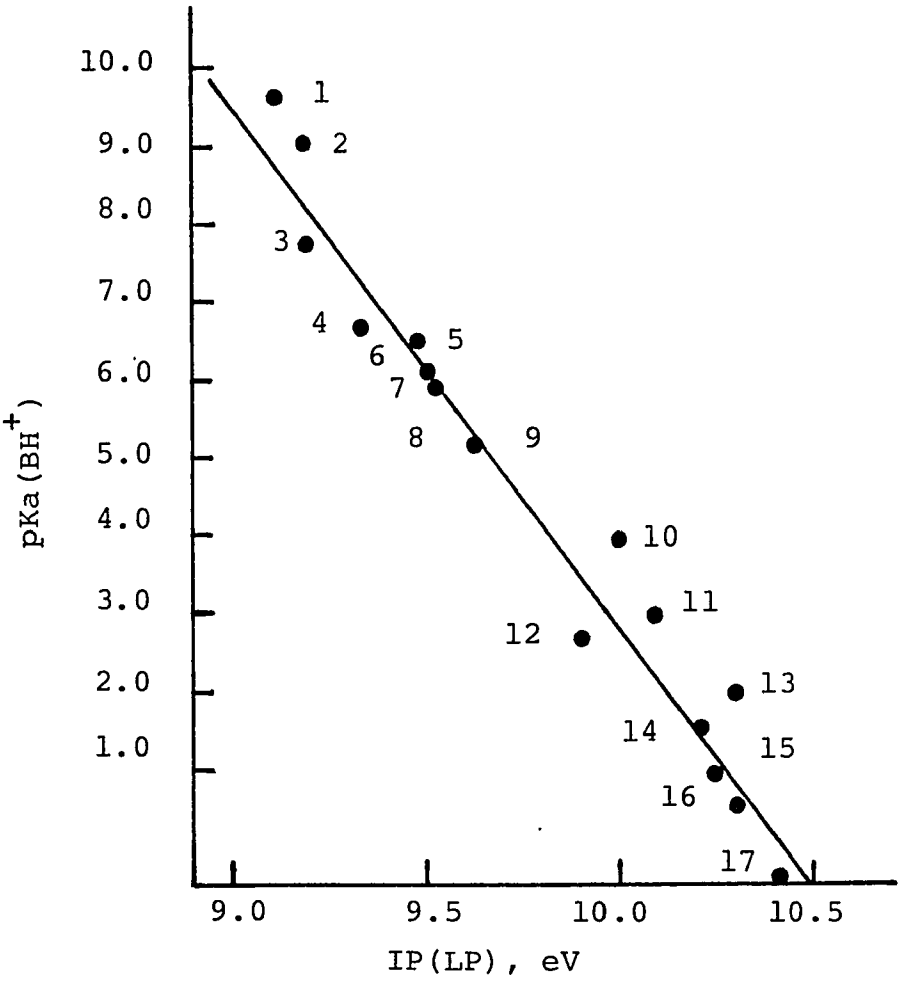

Figure 1. A plot of substituted pyridine pKa's vs. nitrogen lone pair ionization potential: (1) 4-Me_2N, (2) 4-H_2N, (3) 2,4,6-Me_3, (4) 3,4-Me_2, (5) 4-MeO, (6) 3,5-Me_2, (7) 4-Me, (8) 2-Me, (9) H(pyridine), (10) 4Cl, **(11) 3-F** (12) 3-Cl, (13) 4-CN, (14) 3-CN, (15) 3,5-Cl_2, (16) 2-Cl, (17) 2-F

Table 5: Vertical Ionization Potentials (eV) of $Cr(CO)_5L$[a]

L	IP_1[b]	IP_2[b]	IP_3[c]	IP_4[c]
$(C_2H_5)_3P$	7.44[d]	7.58	9.67	11.1[e]
$(CH_3)_3P$[f]	7.58[d]	7.72	10.00	
$(C_2H_3)_3P$	7.52[d]	7.66	9.60	10.33[f]
$(C_2H_5)_2S$	7.45	7.67	9.71	11.48
$(CH_3)_2S$	7.59	7.79	10.00	12.10
$(C_2H_3)_2S$	7.6	7.8	9.48	
$(CH_3)(CH_2Cl)S$	7.74	7.90	10.27	

[a]Reference 10. [b]Assigned to the chromium d orbitals. [c]Assigned to the ligand orbitals with some admixture of metal character. [d]Shoulder. [e]Additional band at 11.3 eV. [f]Assigned to the vinyl groups. Additional ligand bands at 10.76 eV and 12.0 eV.

a_1 (bonding pair) in the pes of the complexes and calculated the energies of stabilization from the uncomplexed ligands (see Table 6).

M. B. Hall[11] and R. F. Fenske[12] have also reported the pes of various other transition-metal complexes $LM(CO)_5$, where M = Cr, Mo or W and L = PEt_3, PMe_3, $P(NMe_2)_3$, $P(OEt)_3$, $P(OMe)_3$, PF_3 and CS (see Table 7). Hall and Fenske placed particular emphasis on the assignment of the metal d orbital band components.* Their relative positions were explained on the basis of differences in backbonding capabilities of the various ligands. However, Lloyd and Hillier[7] have already suggested that the difference in relaxation energy of these orbitals preclude a detailed study of ground state electronic effects.

Before proceeding, to the results of the present investigation, we should consider the band assignments in the pes of the pyridine ligands, since the assignments have produced some controversy.[9,13,14] Table 8 lists the first three IP's of various 4-substituted pyridines. The uncertainty lies in the assignment of the first two bands. However, recent experiments[9,13] support the

---

*The metal bands were deconvoluted using assymetric gaussians.

Table 6: IP_V's (eV) for R_3P and R_2S, and Energies of Stabilization Upon Complexation with the $Cr(CO)_5$ Group[a]

Compound	IP_1	IP_2	Δb_1[b]	Δa_1[b]
$(CH_3)_3P$	8.60[c]	11.3		1.40
$(C_2H_5)_3P$	8.31[c]	10.4		1.36
$(C_2H_3)_3P$	8.51[c]	9.89		1.09
$(CH_3)_2S$	8.69[d]	11.20[e]		0.90
$(C_2H_5)_2S$	8.46[d]	10.70[e]	1.25	0.78
$(C_2H_3)_2S$	8.42[d]		1.06	
$(CH_2)(CH_2Cl)S$	9.17[d]		1.10	

[a]Reference 10. [b]Energy of stabilization upon complexation with $Cr(CO)_5$; $(IP_{COMPLEX}-IP_{BASE})$. [c]Assigned to the lone pair (a_1) orbital. [d]Assigned to the lone pair (b_1)orbital. [e]The other lone pair (a_1) orbital.

Table 7: Vertical Ionization Potentials (eV) of $M(CO)_5L$[a]

Compound	IP_1[b]	IP_2[c]
$Cr(CO)_5PEt_3$	7.6	9.64
$Cr(CO_5)\ PMe_3$	7.6	9.87
$Cr(CO)_5P(NMe_2)_3$	7.6	11.07
$Cr(CO)_5P\ (OMe)_3$	8.0	10.33
$Cr(CO)_5PF_3$	8.7	12.55
$Cr(CO)_5P(OEt)_3$	7.9	10.27
$Mo(CO)_5PEt_3$	7.7	9.63
$Mo(CO)_5PMe_3$	7.7	9.84
$Mo(CO)_5P(NMe_2)_3$	7.8	11.03
$Mo(CO)_5P(OMe)_3$	8.1	10.35
$Mo(CO)_5(PF_3)$	8.8	12.52
$Mo(CO)_5P(OEt)_3$	8.0	10.30
$W(CO)_5PEt_3$	7.8	9.71
$W(CO)_5PMe_3$	7.9	9.92
$W(CO)_5P(NMe_2)_3$	7.9	11.14
$W(CO)_5P(OMe)_3$	8.2	10.36
$W(CO)_5PF_3$	8.9	12.60
$W(CO)\ P(OEt)_3$	8.1	10.34

[a]Reference 11. [b]d-orbitals of metal. [c]Ligand bonding orbital.

Table 8: Vertical Ionization Potentials of $R\text{-}C_5H_4N$ (eV)

R	$IP_1(a_1)$	$IP_2(a_2(\pi))$	$IP_3(b_1(\pi))$
4-H[a]	9.60	9.75	10.50
4-Methyl[a]	9.50	9.60	10.05
4-Ethyl	9.55[b]	9.55[b]	9.98
4-n-Propyl	9.39[b]	9.39[b]	9.57
4-Cl	10.2[c]	10.2	10.2
4-Methoxy	9.3	9.7[d]	> 10.[e]
4-t-Butyl[a]	9.3	9.5	9.7
4-Nitro[f]	10.4	10.48	
4-CF_3[f]	10.1	10.26	11.12
4-Fluoro	10.16[c]		

[a]References 9 and 14. [b]The IP value is for IP_1 and IP_2. [c]This is the center of a broad band. [d]b_1 orbital, the two π orbitals are reversed. [e]a_2 orbital.

assignments of Heilbronner,[14] wherein the first ionization arises from the lone pair (n) orbital on nitrogen and the second and third ionizations are from a_2 and b_1 orbitals respectively (see Figure 2). These latter two π orbitals are derived from the degenerate $e_g(\pi)$ orbitals (9.24 eV)[15] of benzene (see Figure 3) and are further split by the reduced symmetry of pyridine ($D_{6h} \rightarrow C_{2v}$). The stabilization of both orbitals arises from the electronegative nitrogen; the b_1 orbital is stabilized to a greater extent since this orbital has density at the nitrogen ring position. The order, $n(IP_1) < a_2(IP_2) < b_1(IP_3)$ is the one we have adopted.

$b_1(\pi)$ $a_2(\pi)$

Figure 2. Two highest occupied π molecular orbitals of pyridine.

Figure 3. Two highest π molecular orbitals of benzene.

Results and Discussion

Connor and coworkers[16] reported the synthesis of $M(CO)_5L$, (M = Cr, Mo or W and L = any conventional donor such as phosphine or sulfide) from the halopentacarbonylmetallate salt, $R_4N^+[M(CO)_5X]^-$ (R = Me or Et; M = Cr, Mo or W; X = Cl, Br or I). The salt is prepared from the corresponding $M(CO)_6$ and $R_4N^+X^-$ according to the displacement reaction:[17]

$$M(CO)_6 + R_4N^+X^- \rightarrow R_4N^+[M(CO)_5X]^- + CO\uparrow \qquad (3)$$

The salt and ligand, L (L = pyridine), are reacted together in the presence of a Lewis acid (e.g., $Et_3O^+BF_4^-$) to give the monosubstituted product:

$$R_4N^+[M(CO)_5X]^- + L + Et_3O^+BF_4^- \rightarrow M(CO)_5L + R_4N^+BF_4^- + Et_2O + EtX \qquad (4)$$

One of the basic problems in the synthesis is the inability to satisfactorily determine the purity of the halopentacarbonylmetallate salt. Abel and coworkers[17] report the salts to be slightly air and light sensitive. They found solution IR spectra are inconsistent, due to slow decomposition, and their IR spectra were therefore

obtained from KBr discs. However, these spectra gave only very broad peaks. The salt does not melt, but decomposes over a wide range. There are also procedural difficulties. Since the salts are air and light sensitive (particularly when wet or in solution), the synthesis and purification steps must be performed under the darkest possible conditions in an inert atmosphere. When dry, the salts can be handled in the atmosphere for short periods of time.

The complexes ($Cr(CO)_5$:4-RPyridine) could be easily and clearly characterized by their mass spectra, since the initial fragmentation involves only the successive loss of CO groups[18] (except for the t-butyl derivative), without any interfering fragmentation. In all cases the molecular ion peaks were observed, followed by those due to the loss of CO. None of the complexes showed peaks at m/e values higher than the molecular ion. The spectra of the halo and acetyl derivatives showed appreciable amounts of $Cr(CO)_6$, consistent with observations on their photoelectron spectra, but otherwise the spectra were for the most part free of any spurious peaks. The t-butyl derivative had a somewhat more complex spectrum, in that fragmentation corresponded to the loss of a methyl group, followed by the usual loss of CO. The analytical data are listed in Table 9.

Table 9: Analytical Data on $Cr(CO)_5(4\text{-RPyr})$

R	m.p.	%C		%H	
		Calcd.	Found	Calcd.	Found
H[a]	95-97°				
CH_3	101-103°	46.33	46.69	2.47	2.49
$(CH_3)_3C$	108-111°	51.38	51.39	4.00	3.94
CH_3O	97-99°	43.88	44.29	2.34	2.51
Cl[b]	123-125°	39.30	39.16	1.32	1.36
Br	152-155°	34.31	34.63	1.15	1.24
CH_3CO	98-101°	46.02	46.44	2.25	2.18

[a]Reference 19 gives m.p. 95-96°. [b]Reference 20 gives m.p. 128° (dec.).

$Cr(CO)_5$4-RPyridine complexes have a local symmetry of C_{4v} that will split the t_{2g} orbitals of $Cr(CO)_6$ into a b_2 and e set. This symmetry reduction is identical with the case of $Cr(CO)_5NMe_3$,[7,8] where IP_1 and IP_2 were assigned to e and b_2, respectively (see Table 10). The larger peak area for IP_1 vs. IP_2 (see Appendix 2) is also in agreement with Lloyd and Hillier's assignment (see Table 2). The values may be compared with the value of 8.4 eV found for $Cr(CO)_6$,[21] and this represents a significant charge increase at chromium. In fact, all the complexes, with the exception of $Cr(CO)_5$-4-acetylpyridine, have IP's smaller than $Cr(CO)_5NMe_3$ (7.45 eV and 7.76 eV) for e and b_2. Both IP's correlate smoothly with the σ_p values of the substituents, $IP_1 = 0.442\sigma_p + 7.29$, and $IP_2 = 0.446\sigma_p + 7.56$ (see Figure 4). No IP value was more than 0.03 eV from the regression line. The lack of deviation from the standard σ_p correlation, and in particular the lack of any enhanced effect of the methoxy substituent argues against any resonance interaction between the substituents and chromium. The similarity in slope between the correlations involving the e and b_2 orbitals indicate the unimportance of any interaction which would discriminate between these orbitals. This would be true in the ground state as well as in the cation produced by the loss of a d electron. Thus the

Table 10: Vertical Ionization Potentials (eV) of $Cr(CO)_5(4\text{-RPyr})$[a]

R	IP_1[b]	IP_2[b]	IP_3[c]	IP_4[d]	IP_5[e]
CH_3O	7.18	7.45	9.5	9.9	10.3
$(CH_3)_3C$	7.17	7.47	10.17	10.57	11.2
CH_3	7.22	7.48	10.21	10.70	11.24
H	7.30	7.59	10.30	11[g]	11.36[f]
Br	7.37	7.64	10.35[h]		
Cl	7.42	7.66	10.6[h]		
CH_3CO	7.5	7.8			

[a]Reference 22 with adjusted assignments--see text. [b]Assigned to the chromium d orbitals. [c]Assigned to the ring a_2 orbital. [d]Assigned to the ring b_1 orbital. [e]Assigned to the ring a_1 orbital (lone pair). [f]Center of a broad band that is a combination of $b_1(\pi)$ and a_1 lone-pair. [g]IP value is estimated from broad intense bandwidth maximum at 11.36 eV. [h]Center of broad band with shoulder on high energy side. Additional bands at 12.18 eV (chloro compound) and 11.42 eV (bromo compound) assigned to the halogen lone pair.

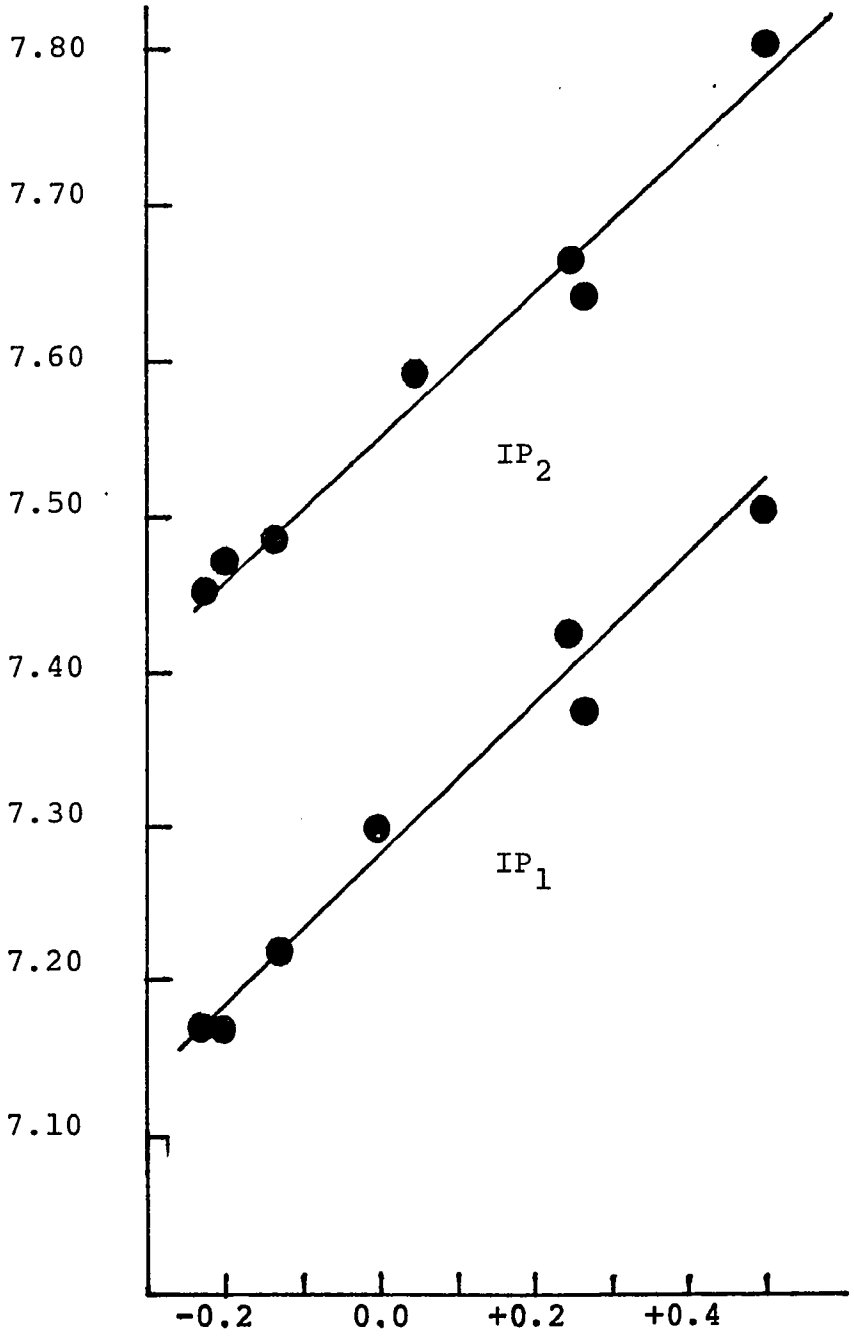

Figure 4. Correlation of IP_1 and IP_2 with the Hammett σ_p.

σ-only model for pyridine ligancy is supported by the analysis of IP_1 and IP_2.

There are three ionization bands below 12 eV due to the pyridine orbitals. These are the a_1 orbital, which contains significant nitrogen lone pair character, and the a_2 and b_1 orbitals. The $b_1(\pi)$ orbital has a large density at the nitrogen and the γ-carbon. It may contain substituent orbital character in many 4-substituted derivatives, as well as in N-substituted derivatives (e.g. various complexes).

In our paper,[22] we originally assigned IP_3 to $a_2(\pi)$, IP_5 to $b_1(\pi)$, with no assignment for IP_4. This assignment of IP_5 to $b_1(\pi)$ appeared somewhat more reasonable at that time than its assignment to IP_4 since the 1 eV separation between a_2 and b_1 π orbitals found for the N-oxides[23,24] and borane complexes[24,25] would also be preserved in the chromium carbonyl complexes. More importantly, it was thought that if the alternative were true (IP_4 is $b_1(\pi)$), the stabilization of the b_1 orbital upon complexation of the methyl- and t-butylpyridines would be hardly more than that found for the a_2 orbital. This would obtain despite the fact that the latter has a nodal plane through positions 1 and 4, and should be considerably less affected by complexation, as observed in the studies on N-oxides and borane complexes. More-

over the implication that IP_4 is then due to an a_1 orbital is poorly founded because of the disturbing lack of such a peak at ca. 11 eV in the pes of the unsubstituted pyridine complex. Finally, we were puzzled by the absence of IP_4 in $Cr(CO)_5$pyridine, estimated to be at 11.0 eV. (The constant relative intensity of IP_4 over a few hours in the spectrometer, measured on several different samples of the methyl and t-butyl complexes, would argue against attribution to an impurity.)

Recently A. Oskam and H. Daaman[8] reported the pes of $Cr(CO)_5$4-RPyridine (R = H, CH_3. $C(CH_3)_3$) with different assignments for the pyridine orbitals (see Table 11). They assigned IP_3 to $a_2(\pi)$, IP_4 to $b_1(\pi)$ and IP_5 to a_1. The more intense and broader fourth band of $Cr(CO)_5$pyridine compared to $Cr(CO)_5$picoline (see Appendix 2) suggested that both IP_4 and IP_5 are part of this band.

As a consequence of the recent work of Oskam, and further studies with BF_3 complexes (to be discussed later), we now support Oskam's assignments. Therefore, in the discussion of the ligand orbitals we have adopted Oskam's assignments.

The first of these IP values (IP_3) in the spectra of complexes of the unsubstituted, methyl and t-butyl derivatives (assigned to the $a_2(\pi)$ orbital) increases by 0.6-0.7 eV upon complexation of the pyridine. This

Table 11: Vertical Ionization Potentials of $M(CO)_5$ imine (eV)[a]

Complex	IP_1[b]	IP_2[c]	IP_3[d]	IP_4[e]	IP_5[f]	IP_6[g]
$Cr(CO)_5$·pyridine	7.29	7.61	10.39	11.46	11.46	
$Cr(CO)_5$·4-picoline	7.29	7.60	10.21	10.72	11.32	
$Cr(CO)_5$·2-picoline	7.28	7.68	9.88	10.91	11.25	
$Cr(CO)_5$·4-t-butylpyridine	7.18	7.51	10.02	10.45	11.26	
$Cr(CO)_5$·2,4-lutidine	7.23	7.49	9.81	10.55	11.09	
$Cr(CO)_5$·4-Cl-pyridine	7.34	7.65	10.52	10.52	11.66	12.23
$Cr(CO)_5$·4-Br-pyridine	7.34	7.67	10.38	10.38	11.37	11.43
$Cr(CO)_5$·pyrazine	7.62	7.93	10.72	-----	-----	10.41
$Cr(CO)_5$·pyridazine	7.22	7.51	11.15	-----	-----	10.28

Complex	IP_1[b,h]	IP_2[c,h]	IP_3[d]	IP_4[e]	IP_5[f]	IP_6[g]
$W(CO)_5$·pyridine	7.29	7.57	10.42	11.41	11.41	
$W(CO)_5$·4-picoline	7.30	7.61	10.22	10.79	11.39	
$W(CO)_5$·4-Cl-pyridine	7.42	7.71	10.59	10.59	11.68	12.24
$W(CO)_5$·4-Br-pyridine	7.38	7.63	10.42	10.42	11.38	11.47

[a]Reference 8. [b]IP_1 is assigned to the metal e orbital. [c]IP_2 is assigned to the metal b_2 orbital. [d]IP_3 is assigned to the $a_2(\pi)$ orbital of imine. [e]IP_4 is assigned to the $b_1(\pi)$ orbital of imine. [f]IP_5 is assigned to the metal-ligand bonding pair. [g]IP_6 is assigned to the other non-bonding pair on the base. [h]IP's of the d-orbitals of $W(CO)_5$ imine corrected for spin-orbit coupling.

compares with the 0.5-0.6 eV increase found for N-oxide formation, and it is less than the 0.8-0.9 eV found for borane complexation. It is much less than the 1.18 eV obtained for boron trifluoride complexation (vide infra). Since the symmetry of a_2 prohibits any direct interaction with the acids, the stabilization of $a_2(\pi)$ is a measure of σ-charge depletion. The alternate possibility for IP_3, assignment to the a_1 orbital, is unlikely because this would mean that upon complexation the a_1 orbital, which is directly involved in the donor-acceptor bond, is stabilized by only 0.7-0.9 eV. This would be less than the stabilization of the two π orbitals, and far short of the 2.2 eV stabilization found by Lloyd for the nitrogen lone pair of NMe_3 in $Cr(CO)_5NMe_3$.[7]

The difference in IP_4 value ($b_2\pi$) between the complexed and uncomplexed pyridine increases with the increasing donor nature of the substituent. A difference of 0.5 eV is obtained upon complexation of the unsubstituted pyridine, if IP_4 is estimated to be at 11 eV. A difference of 0.65 eV is obtained for the 4-methyl derivative and 0.87 eV for the 4-t-butyl derivative.

An interesting contrast is observed with the IP's of the borane complexes. The increase in IP's of the pyridine π orbitals upon complexation with $Cr(CO)_5$ is less than upon BH_3 complexation. This appears especially

true in the case of the b_1 orbital. For instance, ratios of $\Delta b_1/\Delta a_2$ in pyridine-borane and $Cr(CO)_5$pyridine are 1.38/0.88 and 0.5/0.55 respectively (see Table 12). In addition, while the spectra of the 4-halopyridine-boranes show the a_2 and b_1 π IP's as two identifiable separated peaks, the spectra of the chromium complexes show that the whole band envelope is not only shifted to lower energy, but only one broad peak can be seen, with at most a poorly resolved shoulder. This seems due to the small differences in the b_1 IP value between the uncomplexed halopyridine and its chromium carbonyl complex, certainly no more than 0.30-0.60 eV for the chloro complex. (It should be pointed out that the b_1 orbital of the halo derivatives are not localized on the ring but contain considerable halogen character.)

The stabilization of the bonding orbital (a_1) is 1.46 eV for the unsubstituted pyridine and this stabilization increases to 1.74 and 1.9 eV for picoline and t-butylpyridine respectively (see Table 12). This trend is in agreement with the increased donor nature of the bases.

Evidence is presented here, and in the work of Lloyd,[7] that charge donation from amines to $Cr(CO)_5$ exerts less of an effect on the electron energies of the ligand than charge donation to the BH_3 group. However

Table 12: Differences in IP's Between Complexes and Bases[a]

Complex	Δa_2	Δb_1	Δa_1	$\Delta b_1/\Delta a_2$
BH_3·pyridine[b]	0.88	1.38		1.57
BH_3·picoline[b]	0.85	1.36	2.34	1.60
BH_3·ethylpyridine	0.79	1.32	2.10	1.67
BH_3·t-butylpyridine[b]	0.8	1.5		1.87
$Cr(CO)_5$·pyridine	0.55	0.5[c]	1.46[c]	0.9
$Cr(CO)_5$·picoline	0.61	0.65	1.74	1.06
$Cr(CO)_5$·t-butylpyridine	0.67	0.87	1.9	1.29

[a] $IP_{COMPLEX} - IP_{BASE} = \Delta$. [b] From thesis of M. Lattman, Ref. 24. [c] Estimated from fourth ionization band.

an important alternative or perhaps supplementary effect might be present in the $Cr(CO)_5$pyridine system. Recent observations of the d → d transition energies[26,27] and C-O stretchting frequencies[26,27] in a series of complexes $W(CO)_5$:RPyridine shows no evidence that the nature of the substituent on pyridine appreciably influences the electronic nature of the ground state of the $W(CO)_5$ group. More generally, C-O stretching force constants for $M^{VI}(CO)_5$amine complexes appear to be insensitive to the nature of the amines.[28] However M. Wrighton[26] has identified a W → pyridine charge-transfer transition in the electronic spectra of $W(CO)_5$:RPyridine, presumably involving the d orbitals of the tungsten and the π* orbitals of the ring. He has shown that the energy of the charge-transfer transition is quite sensitive to the nature of the ring substituent, decreasing by 0.7 eV from the 4-methylpyridine complex to the 4-acetylpyridine complex. This is due to the increased electron affinity of the ring π* orbitals with electron withdrawing substituents. In addition, Oskam[8] has also reported the ligand field and charge-transfer spectra of $Cr(CO)_5$:RPyridine (R = H, CH_3, t-butyl and Cl) (see Table 4). The ligand field spectra are also insensitive to different substituted pyridines, but the charge-transfer transitions are somewhat sensitive to the nature of the substituent,

decreasing by 2kK from the t-butylpyridine to the 4-Clpyridine complexes. Thus, in the present study, although the pyridine π system is apparently little involved in bonding to chromium in the ground state, the cationic states produced by the loss of a b_1 π electron could be stabilized by charge-transfer from the chromium d orbitals. Recall that transition metal orbitals are extremely sensitive to electronic relaxation (estimated to upwards of 5 eV). Therefore it would only require a small interaction with $b_1(\pi)$ to distort the true values (Koopmans' theorem deviation). Moreover stabilization of the cation would be of decreasing importance with the more electronc donating substituents on the ring, supporting the ΔE trend (and assignment) for the b_1 orbital. Thus symmetry allowed effects, which are deemed unimportant in the ground electronic state of the substituted metal carbonyl systems, could be of increasing importance in the electron deficent cationic states.

In conclusion, the differing values of Δa_2 and Δa_1 obtained suggest that $Cr(CO)_5$ is a weaker acid than BH_3 but this does not fully explain the much greater difference found with Δb_1. Thus it is necessary to invoke the additional factor of a cationic stabilization by $Cr(CO)_5$.

Experimental

Chromium hexacarbonyl was purchased from the Strem Chemical Company and used without further purification. Tetraethylammonium bromide and tetraethylammonium chloride were purchased from the Aldrich Chemical Company and dried over phosphorus pentoxide. R-C_5H_4N (R = H, CH_3, and t-butyl) were purchased from the Aldrich Chemical Company, dried and distilled over calcium hydride. 4-Chloro- and 4-bromopyridine hydrochloride were also bought from the Aldrich Chemical Company. The 4-chloro- and 4-bromopyridines were obtained by adding aqueous KOH to chilled solutions of the corresponding hydrochlorides and extracting the products with ether. The ether solutions were dried and the solvent removed immediately before use. $BF_3 \cdot Et_2O$ was distilled at 39°C (7mm) and stored under prepurified nitrogen. 4-Methoxypyridine was prepared by the reduction of 4-methoxypyridine N-oxide with PCl_3.[29]

Melting points were measured with a Thomas Hoover Capillary Apparatus. Mass spectra were obtained on a Varian CH5 mass spectrometer. Elemental analyses were performed by Galbraith Laboratories, Incorporated, Knoxville, Tennesseee 37921, and Schwarzkopf Microanalytical Laboratory, Woodside, New York 11377.

Typical Synthesis of $Et_4N^+[Cr(CO)_5Br]^-$

This reaction must be carried out under the darkest possible conditions. A mixture of 5.00 g (0.023 mole) of $Cr(CO)_6$, 2.45 g (0.012 mole) of $Et_4N^+Br^-$, and 100 ml of diglyme was placed into a reaction flask fitted with a condenser and an outlet attached to an oil bubbler. The condenser was necessary to catch any $Cr(CO)_6$ which sublimed; the $Cr(CO)_6$ would be pushed back into the reaction mixture by means of a glass rod. The mixture was stirred and heated at 129°C until CO evolution ceased (ca. 2.5 hours). The resulting hot dark orange solution was filtered in an inert atmosphere and then cooled to room temperature. Approximately 100 ml of petroleum ether (b.p. = 36-55°C) was added, and the $Et_4N^+[Cr(CO)_5Br]^-$ precipitated from solution. The solution was filtered off and the salt washed three times with petroleum ether in a dark inert atmosphere. The salt was dried under vacuum to remove petroleum ether, then evacuated at 50°C at 0.01mm to remove any excess $Cr(CO)_6$.

Typical Synthesis of $Cr(CO)_5$pyridine

Under a nitrogen atmosphere, 0.32g of pyridine in 20 ml of methylene chloride was added dropwise to a solution of 0.80g of $Et_4N^+[Cr(CO)_5Br]^-$ and 0.57g of $Et_3O^+BF_4^-$ in 30 ml of methylene chloride. After 30 min. of stirring, all the volatile components were removed with a rotary

mechanical pump. The residue was washed with a 1:1 mixture of hexane-petroleum ether, leaving a crude proudct with a melting point of 92-98^{o}C. Recrystallization from hexane yields a product that melted at 94-97^{o}C. Sublimation at 68^{o}C at 0.01mm sharpens the melting point to 95-97^{o}C.

PART III

UV PES STUDY OF 4-SUBSTITUTED PYRIDINE COMPLEXES OF BF_3 AND BH_3

Background

The bonding interaction of pyridine in Lewis acid-base systems has been of concern in this laboratory.[10,22,23] In view of this, we decided to investigate the pes of a series of substituted pyridine-boron trifluorides. The pes of pyridine-boron trifluoride complexes can be compared to various boron trifluoride-amines[30] and the difference in donor lone pair stabilization may be correlated with their basicities. Moreover, we can compare the stabilization of the a_2 and b_1 π orbitals of pyridine upon complexation with different acids. More importantly, we are now in a position to use the pes data to focus on the relative roles of various acids (BH_3, O-, $Cr(CO)_5$-).

Since a proton is the simplest acid (no steric requirement), we begin with a discussion of proton affinities. Aue and coworkers[31,32] have reported gas phase proton affinity (PA) studies of nitrogenous bases (see Table 13). The proton affinity of pyridine is greater than ammonia, methylamine and ethylamine but less than triethylamine (see Table 13). The charge formed at N^+-H causes an induced dipole in the pyridine

Table 13: Proton Affinities (PA), Vertical Ionization Potentials, Vertical Hydrogen Affinities (vHA) and pKa's of Nitrogen Bases

Base	PA	vIP	vHA	pKa's	% s Character
pyridine[a]	224.8	223.7	134.9	5.17	33
piperidine[a]	230.3	199.7	116.4	11.12	25
ammonia[b]	207	250.2	143	9.26	25
methylamine[b]	218.4	222.8	127	10.657	25
triethylamine[b]	235.5	186.3	108.2	11.01	25
ethylamine[b]	221.4	218.4	126.2	10.807	25

[a]Reference 31. [b]Reference 32.

electrons, leading to a stabilizing effect not found in ammonia, and to a lesser extent with methylamine. However, the large inductive effect of triethylamine more than compensates for the polarizability of pyridine. Aue[31,32] suggested that if the difference in polarizability of the bases can be factored out,[32] the basicity is determined by the hydridization at nitrogen and the trend is similar to solution phase studies of pK_a's (see Table 13). For example, the proton affinities of pyridine $(sp^2N)^*$ and piperidine $(sp^3N)^*$ are 225 and 230 Kcal/mole, respectively. Thus the usual explanation, that the lower basicity of pyridine in solution stems from a hybridization effect, is valid in the gas phase when polarization effects are taken into account. The PA's then show a distinct base weakening effect in compounds with high s character, if comparisons are made where polarizations are canceled. Polarization effects are attenuated in solution (solvents with high dielectric constants).

Since borane and boron halides are more complicated than a proton, the following section will focus on experimental data concerning the basicities of pyridines and alklyamines towards BH_3, BF_3, BCl_3 and BBr_3. Mooney and coworkers[33] have reported the base strength of pyridine to be greater than triethylamine

*It is assumed that the polarization effects will cancel.

towards boron trihalides (BF_3, BCl_3, BBR_3). The authors maintain that the donor ability of a base (or the acceptor ability of an acid) can be correlated with ^{11}B NMR chemical shift data. As the basicity is increased, the electron density at the boron increases, resulting in a greater difference between the ^{11}B chemical shift of the complexed and free boron trihalide ($\Delta\delta$). Table 14 lists the data and shows that the $\Delta\delta$ value for pyridine is consistently greater than the value for triethylamine. This conclusion has been criticized however because ^{11}B chemical shifts are dependent on other factors as well.

Hillier and coworkers[34] measured the core binding energies of the boron 1s orbital in $C_5H_5N \cdot BF_3$ and $C_2H_5NH_2 \cdot BF_3$ by x-ray photoelectron spectroscopy. These investigators suggest that the absolute value of the B 1s orbital energy should reflect the donor ability of the base; the greater the donation, the more destabilized the B 1s orbital (lower binding energy). Their results for the B 1s binding energies of $C_5H_5N \cdot BF_3$ and $C_2H_5NH_2 \cdot BF_3$ are 194.5 eV and 194.8 eV, respectively. This difference of 0.3 eV, they maintain, is enough to indicate that pyridine is a better base. Although conclusions drawn from a difference of 0.3 eV with such large absolute values may be questioned, their conclu-

Table 14: ^{11}B Chemical Shifts (δ) for $C_5H_5N \cdot BX_3$ and $Et_3N \cdot BX_3$ (X = F,Cl,Br) in Acetone Solution[a]

	δ complex[b]		δ acid[b]	$\Delta\delta$[c]	
X	$C_5H_5N \cdot BX_3$	$Et_3N \cdot BX_3$	BX_3	$C_5H_5N \cdot BX_3$	$Et_3N \cdot BX_3$
F	+0.3	-0.2	-9.7	+10.0	+9.5
Cl	-8.0	-10.0	-47.6	+39.6	+37.6
Br	+7.1	+5.1	-40.0	+47.1	+45.1

[a]Table taken from reference 33. [b]ppm from external Me_2OBF_3. [c]$\Delta\delta$ = δ complex - δ acid.

sion is also supported by ab initio and semi-empirical molecular orbital calculations.

In conclusion, the greater basicity of pyridine vs. ethylamine, supported by x-ray photoelectron spectroscopy, agrees with the ordering of their proton affinities. However, Mooney's conclusion that pyridine is a stronger base than triethylamine is not supported by either proton affinities or pK_a's (see Table 13).

The following section focuses on different acids and their pes with similar bases. H. Bock[35] has reported a greater energy of stabilization for the donor lone pair of PF_3 and PMe_3 upon oxidation than upon borane complexation. He concluded that oxygen was the superior σ electron acceptor. Subsequently, Weiner and Lattman[23,24,25] published the corresponding pyridine complexes in which the nitrogen lone pair was not identified.* However, molecular orbital calculations (STO-3G level as well as MINDO/3) showed that the lone pair was stabilized more on N-oxide formation than on borane adduct formation.[24]

The ionization from the a_2 and b_1 (π) orbitals were assigned for both pyridine-N-oxide[23,24] and pyridine-borane[25] (see Tables 15 and 16). It is not unnatural to

---

*Additional substituted pyridine·BH_3 pes will show the donor acceptor pair (see later section).

Table 15: Vertical Ionization Potentials[a] of $RC_5H_4N \cdot BH_3$ (eV)

R	IP_1[b]	IP_2[c]	IP_3
4-CH_3O	9.30	10.5[d]	
4-$(CH_3)_3C$	9.45	10.30	11.21[e]
4-CH_3	9.50	10.45	11.41[e]
4-H	9.72	10.63	11.88[e]
4-Cl	9.71	10.84	11.37[f]
4-Br	9.71	10.82[g]	11.07[f]
4-CF_3	10.04	11.02	12.3[e]
4-NO_2[h]	10.27	11.25	

[a]Ref. 24. [b]BH_3 group. [c]Ring a_2 orbital. [d]IP_2 and IP_3 are unresolved. The value listed is the maximum of the resulting peak. [e]Assigned to the b_1 orbital, largely localized on the ring. [f]Significant admixture of halogen lone pair character. Additional bands at 12.32 (chloro compound) and 11.59 (bromo compound) also assigned to the halongen lone pair. [g]Shoulder. [h]Additional IP's from 11.9-12.5 due to the NO_2 group.

Table 16: Vertical Ionization Potentials (eV) of RC_5H_4N-O[a]

R	IP_1[b]	IP_2[c]	IP_3[d]	IP_4[e]
4-CH_3O	7.89	8.96	10.17	10.54
4-$(CH_3)_3C$	8.00	9.03	9.95	11.00
4-CH_3	8.17	9.09	10.13	11.19
4-H	8.46	9.34	10.36	11.59
4-Cl	8.51	9.48	10.61	-----[f]
4-Br	8.44	9.44	-----[f]	12.24
4-CF_3	8.90	9.76	10.80	12.03

[a]Ref. 24. [b]πO: $(3b_1)$ orbital. [c]σO: (b_2) orbital. [d]πa_2 orbital. [e]$\pi 2b_1$ orbital. [f]Halogen lone pair ionizations interfere.

assume that the stabilization energies of these orbitals would follow the same order as the lone pair orbital (i.e. greater stabilization upon N-oxide formation). Surprisingly, the a_2 (π) orbital showed more than a 50% greater stabilization, and the b_1 orbital ca. a 30% greater stabilization upon borane adduct information. Calculations (STO-3G level) show that the a_2 stabilization is greater for borane adduct formation, but the b_1 stabilizations are similar (see Table 17). In short, it seems that the stabilization of the π orbitals are not following the trend of the greater σ acceptor nature of oxygen. Moreover, this discrepancy is at least as important for a_2 which has a nodal plane through the nitrogen and γ-carbon.

A possible explanation is an orbital interaction between a π component of the acid and the b_1 (π) orbital of pyridine (see Figure 5). The energy of the BH_3 group (e set) is estimated at ca. 10.0 eV from pes studies on alkylamines (or ammonia).[36] Thus the energy condition for orbital interaction is satisfied. This would result in a stabilization of the b_1 (π) of pyridine. However, with the BH_3 tilted away from the pyridine and the e set split by only 0.1 eV, it would seem that the overlap is lacking. In addition, Weiner and Lattman[24,25] did not observe any π interaction between b_1 (π) of pyridine and

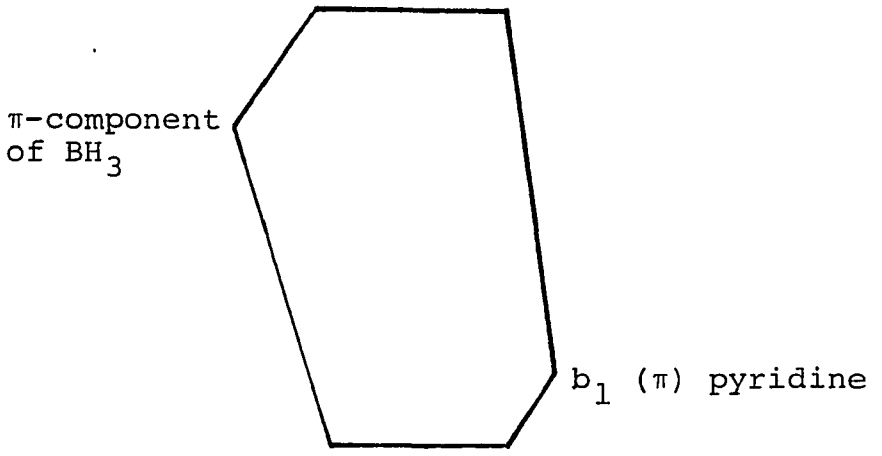

Figure 5. Orbital Interaction Between b_1 (π) of Pyridine and π-Component in BH_3.

Table 17: The Relative Stabilizations (eV)[a] of the RC_5H_4N π Molecular Orbitals Upon N-Oxide Formation and Complexation with BH_3

	Δa_2[b]		Δb_1[b]	
R	N-O	BH_3	N-O	BH_3
4-H	0.61	0.88	1.09	1.38
4-CH_3	0.53	0.85	1.14	1.36
4-$(CH_3)_3C$	0.45	0.8	1.3	1.51
4CF_3	0.54	0.76	0.91	1.18

[a] Ref. 24. [b] $\Delta = IP_{complex} - IP_{base}$.

the e component of BH_3. Therefore, orbital interaction does not seem to be a reasonable explanation. An alternative explanation is a Koopmans' theorem deviation, where the cationic state created by ejection of a b_1 (π) electron (for pyridine-N-oxide) is stabilized by a release of charge from oxygen. However this mechanism cannot explain the small Δa_2 in the N-oxide, where symmetry restrictions prevent any direct interactions.

The greater σ electron donation to oxygen than to BH_3 may be, somewhat ironically, the cause of a compensating trend in the π system. Gross orbital charges, calculated at the STO-3G level, show that although the pyridyl nitrogen σ donor orbital is more severely charge depleted upon N-oxidation than upon BH_3 adduct formation, the opposite is true for the nitrogen p-π orbital. More importantly, this is also true for the α carbons of the pyridine ring, whose p-π orbitals are depleted by ca. 0.16 of a charge unit more in the BH_3 adduct than in the N-oxide. This reversal of donor orbital and π orbital trends is documented elsewhere.[37] Thus, as in the well known case of core electron IP's,[38] the changes in ring π IP values may be correlated with the changes in density at the ring atoms, and while the σ donor IP is increased more upon N-oxidation, the reverse would be true for π orbitals.

An enduring controversy concerns the unexpectedly weak acid character of BF_3 compared to BH_3 and the other boron halides.[39,40] The "expected" observation would have been that the electronegative fluorines of BF_3 cause an increased electron donation from the base upon complex formation, and a greater perturbation of the donor-acceptor electron pair. Despite experiments showing smaller perturbations with BF_3 as the acid, the feeling persists that the lower apparent acidity stems largely from the thermodynamics of formation of the BF_3 complex (see Figure 6).[41]

Traditionally the thinking has been that BF_3 has the larger planar-pyrimidal reorganization energy and the stronger donor-acceptor interaction. Since the reorganization energy (π-breaking) is dominant however, this will lead to a smaller ΔH_f. Drago[42] has suggested an alternate explanation for the weaker acid behavior of BF_3 compared to BCl_3 and BBr_3. He has measured the enthalpies of formation (see Table 18) of various ethyl acetate adducts and their C=O vibrations energies. It was established that the amount of charge depletion caused by the acid is reflected in $\Delta\nu_{C=O}$. He observed a smaller $\Delta\nu_{C=O}$ with BF_3 than BCl_3 or BBr_3, suggesting a smaller charge transfer for BF_3. In Table 14, Mooney et al.[33] have shown that BBr_3 and BCl_3 have a greater ^{11}B shift

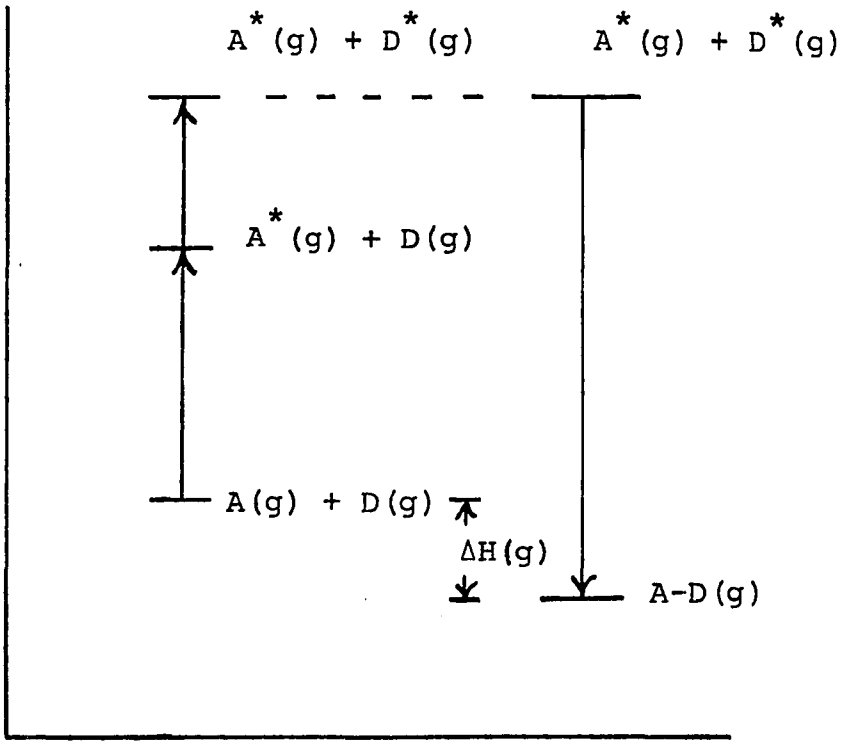

Figure 6. Thermochemical cycle describing adduct formation.

Table 18: Infrared Frequency Shift Measurements for Ethyl Acetate Adducts in CCl_4 Solution[a]

Acid	$\Delta\nu_{C=O}$, cm^{-1}
I_2	26
$(CF_3)_2CHOH$	33
$p\text{-}ClC_6H_4OH$	33
$m\text{-}CF_3C_6H_4OH$	33
HF	33
$(CH_3)_3SiCl$	35
C_6H_5OH	36
$GeCl_4$	36
$SiCl_4$	42
$n\text{-}C_4H_9SnCl_3$	43
ICl	55
$SnCl_4$	90
BF_3	107
$SbCl_5$	138
BCl_3	153
BBr_3	169

[a]Reference 42.

upon complexation with pyridine or triethylamine. This was interpreted as a greater charge donation by the base to BBr_3 and BCl_3 than BF_3. Dipole moment[43] studies of trimethylamine complexes indicate that acceptor power toward that base is in the order $BBr_3 > BCl_3 > BF_3$. D. F. Shriver and B. Swanson[44] have reported that normal coordinate vibrational analyses based on constrained valence fields show that the B-N stretching force constants follow the order $F_3B{\cdot}NCCH_3 < Cl_3B{\cdot}NCCH_3 < Br_3B{\cdot}NCCH_3$ (k(BN) = 2.5, 3.4, and 3.5 mdyn/Å, respectively). The force constants indicate a significantly stronger donor-acceptor bond for BCl_3 than for BF_3. Thus the observed acidity order appears due to less charge donation in the $D{---}BX_3$ bond where BF_3 is the acid.

Results and Discussion

Van der Meulen and Heller[45] reported the earliest preparation of a BF_3· pyridine complex. Boron trifluoride was prepared by heating a mixture of ammonium fluoroborate and boric acid with concentrated sulfuric acid. The BF_3 gas generated was passed into a solution of pyridine in benzene. This was followed by a difficult recrystallization from benzene. More recently, with the commercial availability of BF_3 gas, the gas was bubbled into a solution of pyridine in methylene chloride. This reaction is illustrated in equation 5.

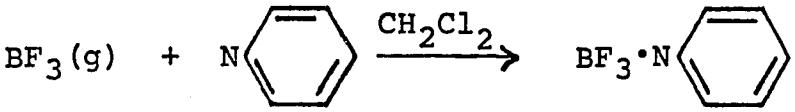

(5)

A constant problem in the preparation was the extreme sensitivity of boron trifluoride complexes to hydrolysis. All substituted pyridines and solvents were dried, carefully distilled over CaH_2 and used immediately. Attempts at sublimation and/or recrystallization (benzene) of the complexes did not improve the melting points and in many instances degraded the complexes. Consequently, the pyridine-boron tribluoride complexes were analyzed and their pes obtained without purification (see Table 19).

Substituted pyridine-boranes were obtained by the nucleophilic displacement of BH_3·SMe_2 by the appropriate base in hexanes. The reaction is illustrated by

Table 19: Analytical Data for BF_3·4-RPyridine and BH_3·4-RPyridine[a]

Complex	M.P.	%C		%H	
		Calcd.	Found	Calcd.	Found
BF_3-pyridine	45-48[b]				
BF_3-picoline	85-89	44.77	44.79	4.38	4.48
BF_3-4-MeOpyridine	85.5-88.5	40.73	40.51	3.99	4.13
BF_3-4-ethylpyridine	56.5-59	48.05	47.96	5.19	5.31
BF_3-4-propylpyridine	45.5-48.5	50.84	50.92	5.87	6.25
BF_3-4-Clpyridine	145-150	33.11	33.20	2.22	2.28
BH_3-4-fluoropyridine	78-80	54.19	54.32	6.31	6.37
BH_3-4-propylpyridine[c]	108°C (.1 mm)	71.16	71.19	10.45	10.48
BH_3-4-ethylpyridine[c]	114°C (.1 mm)	69.49	69.-7	10.00	10.04

[a]All elemental analyses were performed by Schwartzkopf Microanalytical Lab. [b]Literature ref. 49; m.p. = 45°C. [c]These are liquids and the temperatures of distillation are shown.

equation 6.

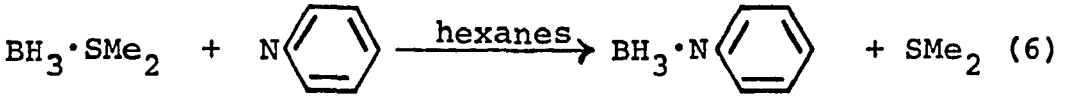

$$BH_3 \cdot SMe_2 + N\langle\bigcirc\rangle \xrightarrow{\text{hexanes}} BH_3 \cdot N\langle\bigcirc\rangle + SMe_2 \quad (6)$$

The boranes complexes were purified by sublimation and their elemental analysis obtained by Schwarzkopf Microanalytical Labs. (see table 19 for results).

The preparation of 4-fluoropyridine and its corresponding BF_3 complex proved extremely difficult. Baudakian[46] has patented a synthetic route to 4-fluoropyridine via the diazotization of 4-aminopyridine in anhydrous hydrogen fluoride. The diazonium ion ($^{+}N_2$-  $NH^{+}F^{-}$) was decomposed to the HF salt of 4-fluoropyridine (F- 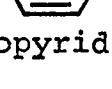 $NH^{+}F^{-}$), and the 4-fluoropyridine can be obtained from the highly acidic fluorination mixture by neutralization in the presence of an organic medium. Addition of HCl(g) will form the stable salt. Because of the difficulty in using anhydrous HF gas in a stainless steel bomb, we modified the reaction by using tetrafluoroboric acid as the fluorinating agent and medium.

The IP values of the 4-substituted pyridine-boron trifluoride complexes are listed in Table 20. The pes of pyridine-boron trifluoride shows three assignable peaks below 13 eV (see appendix 11), and this pattern persists for most of the substituted pyridine-boron trifluorides as well. Exceptions are the methoxy derivative where IP_2 and IP_3 overlap, and the chloro derivative where

Table 20: Vertical Ionization Potentials of $4\text{-}RC_5H_4N\text{-}BF_3$[a]

R	$IP_1(a_2)$	$IP_2(b_1)$	$IP_3(a_1)$
4-H	10.93	11.75	12.39
$4\text{-}CH_3$	10.81	11.12	12.25
$4\text{-}C_2H_5$	10.70	10.90	12.04
$4\text{-n-}C_3H_7$	10.70	10.95	
$4\text{-}CH_3O$	10.35	10.80	
4-Cl	11.17[b]		
4-F	11.42	11.68	12.78

[a]All values in eV. [b]Center of broad band.

ionizations from substitutent orbitals (or orbitals with significant substitutent character) interfere. Since, the pes of BF_3 shows no bands below 15 eV (15.95 eV)[47] these three bands are primarily due to the pyridine.

MNDO[48] and CNDO/S[49] semi-empirical calculations were obtained to help in the assignments and the interpretation of ionization band shifts. MNDO was chosen because the program was parameterized to handle a perfluoro group.[47] It was tested with BF_3 and the eigenvalues (16.33 eV) of the degenerate HOMO set are similar to the IP's in the pe spectrum. To minmize the number of variables optimized, all substituted pyridines, BH_3-pyridine complexes and BF_3-pyridine complexes used the same bond lengths and bond angles as in pyridines. However, for the substituted pyridines, the substitutent "bond" to the para carbon was optimized, and in the complexes the two variables optimized were (1) F-B-F or H-B-H angle and (2) B-N bond length. The final optimized geometries are shown in Table 21. In addition, CNDO/S calculations were also obtained to support the MNDO results. The CNDO/S was used because it is parameterized specifically for spectroscopic data and to handle perfluoro groups (MINDO, CNDO, PRDDO and ab initio calculations at the STO-3G level place the perfluoro group orbitals at much too high in energy).

The first ionization band (IP_1 = 10.93 eV) in BF_3·pyridine is from an $a_2(\pi)$ orbital. This orbital

Table 21: Optimized Geometries for BH_3 and BF_3 Complexes Using MNDO

Complexes	B-N[a]	X-B-X[b]	B-X[c]
BH_3·pyridine	1.5936	106.59	1.21
BH_3·picoline	1.5937	106.61	1.21
BF_3·pyridine	1.6616	107.31	1.43
BF_3·picoline	1.6626	107.27	1.43

[a]B-N bond distance in angstroms. [b]X-B-X (X = H or F) bond angle. [c]B-X (X = H or F) were held constant.

has a nodal plane through the nitrogen and para carbon. The assignment is supported by the HOMO of both MNDO and CNDO/S calculations (see tables 22 and 23). The experimental increase in energy of a_2 upon complexation (Δa_2) is 1.18 eV, and this stabilization is larger than the corresponding values of 0.88 eV in BH_3·pyridine, 0.61 eV in pyridine-N-oxide and 0.55 eV in $Cr(CO)_5$·pyridine (see table 24). The relative ordering is supported by MNDO calculations where the a_2 increases are 1.59 eV in BF_3·pyridine, 1.18 eV in BH_3·pyridine, and 0.83 eV in pyridine-N-oxide (see table 25). For the other BF_3·4-RPyridine complexes (R=CH_3, C_2H_5, and F), the a_2 values upon complexation are similar to BF_3·pyridine, clustering around 1.2 eV. This clustering of the Δa_2 values found in BF_3 complexes is also observed in BH_3·4-RPyridine complexes (R = H, CH_3, C_2H_5,) and pyridine N-oxides (see table 17).

The second ionization band (IP_2 = 11.75 eV) in BF_3·pyridine is from a b_1 (π) orbital. This assignment is also supported by the ordering found in MNDO and CNDO/S calculations (see tables 22 and 23). The experimental b_1 (π) increase is 1.25 eV in BF_3·pyridine and this stabilization is smaller than 1.38 eV in BH_3 pyridine but larger than 1.09 eV in pyridine-N-oxide, and 0.5 eV in $Cr(CO)_5$·pyridine. Even more startling is the Δ b_1 (π) trend obtained within the series of BF_3·4-RPyridine (R = H, CH_3, C_2H_5). The Δb_1 (π) IP decreases from 1.25 in eV

Table 22: MNDO Eigenvalues (eV)

Compounds	a_1(lone pr.)	$b_1(\pi)$	$a_2(\pi)$
Pyridine	-11.02607	-10.52231	-9.69270
Picoline	-11.08145	-10.45805	-9.74906
4-Ethylpyridine	-11.00437	-10.44288	-9.82095
4-Fluoropyridine	-11.49640	-10.69824	-10.27669

	$a_1(\sigma)$	b_1(ring)	BH_3(gp.)	a_2(ring)	b_1(BH_3 group)
Pyridine·BH_3	-13.39945	-12.29113	-11.08939	-10.87307	-10.59552
4-Picoline·BH_3	-13.26305	-12.03641	-11.06659	-10.83564	-10.53077
4-Ethylpyridine·BH_3	-13.09207	-11.99582	-11.05806	-10.82393	-10.51641
4-Fluoropyridine·BH_3	-13.99909	-12.27594	-11.28648	-11.28571	-10.75765

	$a_1(\sigma)$	$b_1(\pi)$	$a_2(\pi)$
Pyridine·BF_3	-13.29655	-12.31259	-11.28472
4-Picoline·BF_3	-13.22883	-12.01404	-11.23794
4-Ethylpyridine·BF_3	-13.16265	-11.96730	-11.22094
4-Fluoropyridine·BF_3	-13.61900	-12.26254	-11.68796

Compounds	$b_1(\pi)$	$a_2(\pi)$
Pyridine N-oxide	-12.42917	-10.52419

Table 23: CNDO/S Eigenvalues Using Optimized Bond Lengths and Angles (eV)

Complexes	$a_2(\pi)$	$b_1(\pi)$	$a_1(n)$
Pyridine	-10.7780	-11.8668	-12.2527
Picoline	-10.7863	-11.4864	-12.1017
Pyridine-BH_3	-12.0056	-13.9711	-14.01554
Picoline-BH_3	-11.947474	-13.467257	-13.76682
Pyridine-BF_3	-12.2507	-13.5471	-14.1324
Picoline-BF_3	-12.1838	-12.979	-13.8913

Table 24: Differences in IP's Between Complexes and Bases[a]

Complexes	Δb_1	Δa_2	Δa_1	$\Delta b_1/\Delta a_2$
Pyridine·BH_3[b]	1.38	0.88		1.57
Picoline·BH_3[b]	1.36	0.85	2.34	1.60
Ethylpyridine·BH_3	1.32	0.79	2.10	1.67
Pyridine·BF_3	1.25	1.18	2.79	1.06
Picoline·BF_3	1.07	1.21	2.75	0.9
Ethylpyridine·BF_3	0.92	1.15	2.49	0.8
$Cr(CO)_5$pyridine	0.5	0.55	1.5	0.9
$Cr(CO)_5$picoline	0.65	0.61	1.74	1.06
$Cr(CO)_5$-4-butylpyridine	0.87	0.67	1.9	1.29
Pyridine-N-oxide[b]	1.09	0.61	0.61	1.78

[a]In eV. [b]Reference 24.

Table 25: MNDO Stabilizations

Compounds	Δa_1	Δb_1	Δa_2	$\Delta b_1/\Delta a_2$
BH_3·pyridine	2.363	1.76	1.18	1.5
BH_3·picoline	2.182	1.57	1.08	1.45
BH_3·ethylpyridine	2.09	1.55	1.00	1.55
BF_3·pyridine	2.270	1.79	1.59	1.1
BF_3·picoline	2.14	1.55	1.48	1.05
BF_3·ethylpyridine	2.16	1.52	1.40	1.1
Pyridine N-oxide		1.90	0.83	2.28

in BF_3·pyridine to 1.07 eV in BF_3·picoline and 0.92 eV in BF_3·ethylpyridine, as the substituent becomes more electron donating. This trend can be compared with the slight decreasing Δb_1 (Δ) stabilization observed in BH_3·pyridine, BH_3 picoline, and BH_3 ethylpyridine (1.38 eV, 1.36 eV and 1.32 eV)* (see Table 24).

The third ionization band observed in the BF_3·pyridine complexes are assigned to the bonding electron pair (a_1). This band is resolved in the pyridine, picoline, ethylpyridine, and fluoropyridine boron trifluoride complexes, but is not resolved in the propyl, methoxy and chloropyridine complexes (see Table 20). Table 24 gives the calculated a_1 increases upon complexation. There is no relationship between increasing donor electron energies (lower IP's) of the pyridine bases and their magnitude of stabilization (Δa_1) in the BF_3·pyridine complexes. Comparisons with trimethylamine and dimethylamine boron trifluorides are inconclusive. The a_1 values upon complexation are 3.7 eV and 3.2 eV for BF_3·NMe_3 and BF_3·NMe_2H respectively.

In an attempt to compare the acidity of BH_3 and BF_3, we wanted to investigate the stabilization of the bonding electron pair upon complexation with BH_3. Lattman and Weiner[24,25] did not report the donor lone pair in the spectra of BH_3·pyridine complexes. However, it was noticed that IP_3 (assigned to $b_1(\pi)$, see Appendix 11)

* Δ values have a ± 0.04 uncertainty.

in picoline-borane had a shoulder on the higher ionization energy side of the band. Therefore, the pes of some additional substituted pyridine-boranes (C_2H_5, F, and n-C_3H_7) were obtained (see Table 26), and the fourth IP was resolved in the former two complexes.

The following discussion will focus on the difference in charge densities upon complexation with the two acids. These differences will be utilized to explain the Δa_2 (π) trend obtained in the pes results. Tables 27-32 list the calculated total, π, and σ charge densitites (MNDO and CNDO/S) of pyridine, picoline, and their corresponding BH_3 and BF_3 complexes.

MNDO calculations show that the nitrogen atom in pyridine is more charge depleted when forming a borane adduct (-0.218 charge)* than a boron trifluoride complex (-0.095 charge)*. The σ density on nitrogen is similarly depleted (see Table 27, 28, and 29). MNDO shows that the corresponding picoline complexes follow the same trend as well (see Tables 30, 31, and 32).

In contrast to the σ depletion (or as compensation for it), the calculations show that at the nitrogen, the π charge density increases upon complexation. For example, in BF_3·pyridine the π charge increase at nitrogen of +0.174 is larger than the +0.101 charge increase in BH_3·pyridine. Ironically, the nitrogen atom in

---

*total charge density at N in complex -total charge density at N of pyridine.

Table 26: Vertical Ionization Potentials of R-C_5H_4N-BH_3

R	IP_1[a]	IP_2[b]	IP_3[c]	IP_4[d]
4-CH_3O[e]	9.30	10.5		
4-t-Butyl[e]	9.45	10.30	11.21	
4-CH_3[e]	9.50	10.45	11.41	11.8 (shoulder)
4-H[e]	9.72	10.63	11.88	
4-Cl[e]	9.71	10.84	11.37	
4-Br[e]	9.71	10.82	11.07	
4-CF_3[e]	10.04	11.02	12.3	
4-NO_2[e]	10.27	11.25		
4-Ethyl	9.51	10.34	11.30	11.65
4-n-Propyl	9.46	10.33	11.17	
4-Fluoro	9.84	10.93	11.81	12.28

[a]Band due to BH_3 group orbitals. [b]IP_2 is an ionization from an $a_2(\pi)$ orbital. [c]IP_3 is an ionization from a $b_1(\pi)$ orbital. [d]IP_4 is an ionization from the acceptor-donor orbital. [e]From reference 24.

Table 27: Calculated Charge Densities for Pyridine

	MNDO	CNDO/S
N[a]	5.21476	5.375273
π[b]	1.15376	
σ[c]	4.06100	
C_o[d]	3.94899	3.814480
π	.91132	
σ	3.03767	
C_m[e]	4.12509	4.111073
π	1.04274	
σ	3.08235	
C_p[f]	4.00695	3.948229
π	.94001	
σ	3.06694	
C_m[e]	4.12559	4.111994
π	1.04238	
σ	3.08321	
C_o[d]	3.94837	3.814752
π	.90979	
σ	3.03858	

[a]Total charge at nitrogen. [b]π charge at nitrogen. [c]σ charge at nitrogen. [d]Ortho carbons. [e]Meta carbons. [f]Para carbon.

Table 28: Calculated Densities for BF_3·pyridine

	MNDO	ΔMNDO[a]	CNDO/S	ΔCNDO/S[b]
N[c]	5.11924	-0.09552	5.173913	-0.20146
π[d]	1.32823	+0.17447		
σ[e]	3.79101	-0.26999		
C_o[f]	3.87568	-0.07331	3.793775	+.020705
π	.86044	-0.05088		
σ	3.01524	-0.02243		
C_m[g]	4.11623	-0.0088	4.104955	0.006118
π	1.03519	-0.00755		
σ	3.08104	-0.00131		
C_p[h]	3.95833	-0.04862	3.91135	-0.036879
π	.87483	-0.06518		
σ	3.0835	+0.0166		
C_m[g]	4.11637	-0.00922	4.105085	-0.006909
π	1.03534	-0.00703		
σ	3.08103	-0.00218		
C[f]	3.87545	-0.07292	3.793336	-0.021416
π	.86005	-0.04974		
σ	3.0154	-0.02318		

	MNDO	ΔMNDO[a]	CNDO/S	ΔCNDO/S[b]
B	2.59142		2.263704	
	.57200			
	2.01942			

---

[a] $\Delta MNDO = MNDO_{complex} - MNDO_{base}$. [b] $\Delta CNDO/S = CNDO/S_{complex} - CNDO/S_{base}$. [c] Total charge at nitrogen. [d] π charge at nitrogen. [e] σ charge at nitrogen. [f] Ortho carbons. [g] Meta carbon. [h] Para carbon.

Table 29: Calculated Charge Densities for BH_3·pyridine

	MNDO	ΔMNDO[a]	CNDO/S	ΔCNDO/S[b]
N[c]	4.99623	-0.21853	5.027452	-0.350821
π[d]	1.25873	+0.10497		
σ[e]	3.7375	-0.3235		
C_o[f]	3.90899	-0.0401	3.82850	-0.01402
π	0.89384	-0.01748		
σ	3.01506	-0.02261		
C_m[g]	4.11094	-0.01415	4.096306	-0.014767
π	1.03228	-0.010		
σ	3.07866	-0.00369		
C_p[h]	3.98304	-0.02391	3.932580	-0.015649
π	0.90496	-0.03505		
σ	3.07808	+0.01118		
C_m[g]	4.11076	-0.01483	4.095869	-0.016125
π	1.03246	-0.00992		
σ	3.0783	-0.00491		
C_o[f]	3.90882	-0.03955	3.827834	+0.013082
π	0.89480	-0.01499		
σ	3.01402	-0.02436		

	MNDO	ΔMNDO[a]	CNDO/S	ΔCNDO/S[b]
B	3.18140		3.171697	
π	0.77088			
σ	2.41052			

---

[a] $\Delta MNDO = MNDO_{complex} - MNDO_{base}$. [b] $\Delta CNDO/S = CNDO/S_{complex} - CNDO/S_{base}$. [c] Total charge at nitrogen. [d] π charge at nitrogen. [e] σ charge at nitrogen. [f] Ortho carbons. [g] Meta carbons. [h] Para carbon.

Table 30: Calculated Charge Densities for Picoline

	MNDO	CNDO/S
N[a]	5.20464	5.390388
π[b]	1.14971	
σ[c]	4.05493	
C_o[d]	3.95190	3.800828
π	0.90903	
σ	3.04287	
C_m[e]	4.10746	4.146093
π	1.03685	
σ	3.07061	
C_p[f]	4.05450	3.864571
π	0.95674	
σ	3.09776	
C_m[e]	4.10582	4.140235
π	1.03904	
σ	3.06678	
C_o[d]	3.95716	3.807021
π	0.91703	
σ	3.04013	
C[g]	3.92762	4.109153
π	0.92054	
σ	3.00708	

[a]Total charge density at nitrogen. [b]π charge density at nitrogen. [c]σ charge density at nitrogen. [d]Ortho carbons. [e]Meta carbons. [f]Para carbon. [g]Methyl carbon at 4 position.

Table 31: Calculated Charge Densities for BF_3·picoline

	MNDO	ΔMNDO[a]	CNDO/S	ΔCNDO/S[b]
N[c]	5.11924	-0.0854	5.189193	-0.2011
π[d]	1.32983	+0.18016		
σ[e]	3.78941	-0.26852		
C_o[f]	3.87647	-0.07543	3.785603	-0.0152
π	0.86127	-0.04776		
σ	3.0152	-0.0276		
C_m[g]	4.10272	-0.00474	4.137187	-0.0089
π	1.03439	-0.002		
σ	3.06833	-0.00223		
C_p[h]	4.00366	-0.05084	3.833956	-0.0306
π	0.88602	-0.07072		
σ	3.11764	+0.04		
C_m[g]	4.10397	-0.00185	4.137657	-0.0025
π	1.03516	-0.00388		
σ	3.06881	+0.002		
C_o[f]	3.87641	-0.080	3.786729	-0.0202
π	0.86139	-0.0336		
σ	3.01502	-0.025		

	MNDO	ΔMNDO[a]	CNDO/S	ΔCNDO/S[b]
B	2.59208			
π	.57195			
σ	2.02013			
C[i]	3.94004		4.107542	
π	.93523			
σ	3.00481			

[a] $\Delta MNDO = MNDO_{complex} - MNDO_{base}$. [b] $\Delta CNDO/S = CNDO/S_{complex} - CNDO/S_{base}$. [c] Total charge at nitrogen. [d] π charge at nitrogen. [e] σ charge at nitrogen. [f] Ortho carbons. [g] Meta carbons. [h] Para carbon. [i] Methyl carbon.

Table 32: Calculated Charge Densities for BH_3·picoline

	MNDO	ΔMNDO[a]
N[b]	4.99609	-0.20855
π[c]	1.25926	+0.10955
σ[d]	3.73683	-0.3211
C_o[e]	3.90999	-0.04191
π	0.89495	-0.01408
σ	3.01504	-0.0278
C_m[f]	4.09685	-0.0106
π	1.03055	-0.006
σ	3.0663	-0.00431
C_p[g]	4.02920	-0.0253
π	0.91746	-0.03918
σ	3.11174	+0.034
C_m[f]	4.09668	-0.009
π	1.03073	-0.008
σ	3.06595	-0.0008
C_o[e]	3.90992	-0.047
π	0.89591	-0.021
σ	3.01401	-0.020

	MNDO	ΔMNDO[a]
B	3.18132	
π	.77064	
σ	2.41068	
C[h]	3.93443	
π	0.93056	
σ	3.00387	

[a]$\Delta MNDO = MNDO_{complex} - MNDO_{base}$. [b]Total charge density at nitrogen. [c]π charge at nitrogen. [d]σ charge at nitrogen. [e]Ortho carbons. [f]Meta carbons. [g]Para carbon. [h]Methyl carbon at 4 position.

BF_3·pyridine is less σ charge depleted yet is compensated to a larger extent at the π level. This charge build up at the p-π orbital of nitrogen is at the expense of the ortho ring carbons (see Table 28). More importantly, the π orbital charge depletion at the ortho positions is over three times greater in BF_3·pyridine than in BH_3·pyridine. It is precisely the difference in π charge depletion at the ortho ring positions that accounts for the relative Δa_2 stabilization in the BF_3 and BH_3 complexes. The magnitude of Δa_2 can be attributed to the total amount of charge depletion, and particularly the movement of π charge at the ortho and meta positions. The larger Δa_2 obtained in BF_3·pyridine (1.18 eV) than in BH_3·pyridine (0.88 eV) can be explained by the greater relative charge depletion at the ortho carbon π orbitals.

It would seem inconsistent that the larger π polarization (BF_3·pyridine) is obtained with nitrogen that is less charge depleted. However, MNDO also indicates a large positive charge (+0.401) developed at the boron atom in BF_3·pyridine whereas in pyridine-borane there is a negative charge (-0.18) at the boron. The positive charge formed at boron in BF_3·pyridine is caused by the electronegative fluorines which are responsible for the severely alternating charge, negative at fluorines and positive at boron, and for the consequent polarization in the π system.

The $\Delta b_1(\pi)$ stabilizations for BH_3 and BF_3 complexes are inherently more difficult to interpret than the $\Delta a_2(\pi)$. Symmetry does not preclude orbital interactions with the π components of para substituents (CH_3 or C_2H_5) or acids. Consequently, the simple explanation utilized (changes in charge densities) in explaining Δa_2 upon complexations is inadequate to justify the stabilizations of $b_1(\pi)$. (1) The ratio of experimental $\Delta b_1/\Delta a_2$ for pyridine and picoline complexes of BF_3 are 1.1 and 0.9 eV respectively (see table 24). This compares favorably with the MNDO calculated $\Delta b_1/\Delta a_2$ ratio of 1.1 and 1.05 eV obtained for the corresponding complexes (see table 32). (2) The experimental ratio $\Delta b_1/\Delta a_2$ for pyridine and picoline borane complexes are 1.6 and 1.6 eV respectively (see table 24). The MNDO calculated ratio for the corresponding complexes are 1.5 and 1.45 eV respectively (see table 32). (3) In general the $\Delta b_1/\Delta a_2$ ratios are 50% greater for BH_3 than BF_3. This trend is observed experimentally as well as by MNDO calculations. Since, MNDO (ground state calculations) support the experimental results, this difference cannot be attributed to differences in relaxation effects. (4) For the electron-donating substituents, the Δb_1 stabilizations decrease moderately in the borane and more steeply in the boron trifluoride complexes. (The Δb_1 increases observed in $Cr(Co)_5 \cdot$4-R Pyridine may be anomalous. The trend is in reversed because of d orbital relaxation effects). The

$b_1(\pi)$ orbital is destabilized in picoline and ethylpyridine by orbital interaction with a π component in the alkyl group. The $b_1(\pi)$ ring orbital interacts in an antibonding fashion resulting in a nodal region between the para carbon and substituent carbon (almost 7% of the $b_1(\pi)$ ring density in picoline can be found on the methyl substituent). Upon complexation a (+N≡) positive center is formed at the nitrogen and this cationic site will stabilize the $b_1(\pi)$ orbital. However, in the case of picoline-BF_3 some of the $b_1(\pi)$ density (approximately 10%) is on the methyl substituent and so constrained in that region that it will not feel the cationic site. Consequently, though the $b_1(\pi)$ of picoline is higher in energy, because of the additional nodal region caused by methyl interaction the charge (e^-) ($b_1(\pi)$ CH_3) will be isolated from the cationic nitrogen.

It is also noted that the $\Delta b_1(\pi)$ trend increases from 1.09 to 1.13 to 1.3 eV in going from O-N⟨◯⟩, O-N⟨◯⟩ - CH_3 to O-N⟨◯⟩ -t-bu respectively. However, MNDO calculations show that there is a significant oxygen (π) to $b_1(\pi)$ ring interaction that would lend to a $b_1(\pi)$ stabilization. In fact 16% of the $b_1(\pi)$ ring orbital (by charge density) is found on the oxygen and this interaction (stabilizing $b_1(\pi)$) will dominate the <u>substituent effect</u>. In BF_3 and BH_3, there is neglible π interaction from the acid.

The experimental increase in the a_1 (bonding pair) IP upon complexation to the BF_3·picoline (2.79 eV) is larger than BH_3·picoline (2.39 eV). However, MNDO calculations show the reverse ordering; BH_3·picoline (2.18 eV) has a larger a_1 stabilization than BF_3·picoline (2.14 eV) (see Table 31). In the two complexes the nature of the a_1 (bonding orbital) is vastly different in character. In BH_3·picoline only 20% (by charge density) of the orbital is located on BH_3 while in BF_3·picoline about 50% of it is located on the fluorine atoms. Many of the semi-empirical calculations do not handle perfluoro groups well. The consequent exaggerated fluorine character in a_1 may raise the eigenvalue too high in the BF_3 complex. The CNDO/S calculations on the a_1 stabilization are in agreement with the pes results with regard to a a_1 stabilization. However, CNDO/S reveals only a 15% contribution from the fluorine orbitals. Consequently the eigenvalue calculated for the a_1 orbital in BF_3·picoline is not saddled with difficulty of perfluoro character. (Otherwise CNDO/S results on the π orbitals by and large mimic the MNDO picture. They show a greater charge depletion at the nitrogen in BH_3·pyridine (-0.350 charge) than BF_3·pyridine (-0.201 charge). In addition, CNDO/S reveals a large positive charge formed at boron in BF_3·pyridine.)

In summary, an important difference between BF_3 and BH_3 complexes with pyridine is the former's ability to polarize π electrons in the ring towards nitrogen. The origin of this effect can be traced to the electronegative fluorines pulling charge away from boron. The positive boron can now induce polarization in the π electron system.

Conclusion

There are potentially four factors that determine the magnitude of Δa_2 and Δb_1 (π) stabilization upon complexation; (1) charge depletion caused by complexation; this factor is always present, (2) orbital interactions that can directly affect b_1 (π) and indirectly perturb a_2 (π), (3) a Koopmans' theorem deviation, and (4) a polarization of the π system.

In the $Cr(CO)_5$ pyridine system, there was little evidence for backbonding from Cr d orbitals in the ground state, but there is a likelihood of charge transfer in an ionic state (caused by ejection of a $b_1(\pi)$ electron). This conclusion was based upon observation of a destabilized b_1 (π) upon complexation, especially with electron withdrawing substituents on pyridine. This observation was also supported by the electronic charge-transfer bands that showed their energies to be sensitive to the nature of the substituents on pyridine.

In the BH_3·pyridine system, the calculations (MNDO and CNDO/S) predict some orbital interaction between a π component of BH_3 and the b_1 (π) in pyridine. The stabilization in b_1 (π) orbital energy upon complexation can be rationalized by this interaction and by charge

depletion. However, pes results did not show any splitting of the BH_3 group orbitals into a π and σ component in the complexes. This is evidence against orbital interaction.

In the BF_3·pyridine system, the calculations indicate no orbital interaction between the BF_3 group and b_1 (π) on the ring.* However, the π electrons are strongly polarized towards the nitrogen atom. The cause of this polarization is the electronegative fluorines creating a large positive charge at boron. This factor, in conjunction with charge depletion determines the magnitude of Δa_2.

In the pyridine-N-oxides, MNDO calculations show a large π interaction between the p-π orbital on oxygen and b_1 (π) on the ring.[25] This interaction will stabilize the b_1 (π) but destabilize the a_2 (π). Calculations suggest that this interaction sends a net π charge back into the ring neutralizing the σ flow from nitrogen and resulting in smaller Δa_2 but relatively larger Δb_1.

Finally, it is worthwhile to mention that a deeper understanding of the acid-base interaction of pyridine was only realized when several systems were compared, in conjuction with the calculations.

---

*Over 98% of the charge density is found on the pyridine ring (charge density is obtained by squaring the orbital coefficients).

Experimental

Boron trifluoride gas was purchased from Matheson Co. and used without further purification. 4-Aminopyridine was bought from Aldrich Chemical Company and recrystallized from acetone. 4-Ethylpyridine was purchased from Aldrich Chemical Co. and dried and distilled over CaH_2. All other substituted pyridines were treated as above (see previous experimental section). Borane-methyl sulfide complex, 10.0M in BH_3 (neat liquid, contains ca. 5% excess methyl sulfide) was purchased from Aldrich Chemical Co. Tetrafluoroboric acid 48% was purchased from Alfa Inorganics (Ventron).

Melting points were measured with a Thomas Hoover Capillary Apparatus. Mass spectra were obtained on a Varian CH5 and AEI MS902. Elemental analysis was performed by Schwarzkopf Microanalytical Laboratory, Woodside, New York 11377.

Typical Synthesis of 4-Clpyridine·BF_3

4-Chloropyridine hydrochloride was basified with aqueous KOH at ice-bath temperature, and was extracted into pentane. The pentane solution was dried with $MgSO_4$ and then over molecular sieves (type 4A). The solvent was removed, and 4-chloropyridine was distilled at 40°C (10 torr). Boron trifluoride gas was added to a chilled hexane solution of 4-chloropyridine, resulting in a white precipitate. The precipitate was washed three times with hexane and dried under vacuum, m.p. 145-150°C.

Typical Preparation of 4-Fluoropyridine Hydrochloride

20g (0.21 mole) of 4-aminopyridine was dissolved in 80 ml of tetrafluoroboric acid (48%) in a 500 ml flask. The reaction mixture was kept between -10 and +10°C during the slow addition (45 min.) of 14.7g (0.21 mole) of $NaNO_2$. The 4-pyridyldiazonium fluoride was then decomposed at 30-50°C over a 1.5 hr. period. After the decomposition was complete (cessation of gas evolution), the reaction mixture was cooled to -10°C and transferred to a cold (-10°C) neutralization vessel containing 29% ammonium hydroxide (50 ml) and methylene chloride (200 ml). The methylene chloride layer was separated and dried over $MgSO_4$. Hydrogen chloride gas was passed into the

methylene chloride solution of 4-fluoropyridine, and the methylene chloride was removed at ambient temperatures to give a yellowish solid with a melting range from 100-120°C. The residue was dissolved into hot chloroform and hot filtered. Hexane was added to precipitate the 4-fluoropyridine hydrochloride from chloroform. The white precipitate was dried under vacuum and had a sharp melting pt. 121-123°C. The melt evolved a gas (HCl), followed by formation of a dark orange solid (quaternization). The 4-fluoropyridine·BF_3 was prepared similarly to the synthesis of 4-chloropyridine·BF_3.

Typical Synthesis of 4-Ethylpyridine·BH_3

Excess dimethylsulfide-borane was added to a chilled solution of 4-ethylpyridine in pentane. The excess dimethylsulfide-borane (97°c, 760 torr), pentane and dimethylsulfide were removed under vacuum. The liquid residue was distilled at 114°C (0.1 torr).

PART IV

UV PES STUDY OF BORANE-N-SUBSTITUTED IMIDAZOLE COMPLEXES

Results

N-substituted imidazoles (I) and the corresponding BH_3 and BF_3 complexes (II) (where R = H, CH_3, C_2H_5, and n-C_4H_7) were chosen to test the ideas developed in the previous section on substituted pyridine complexes.

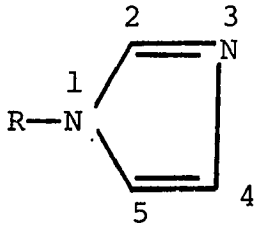

(I)

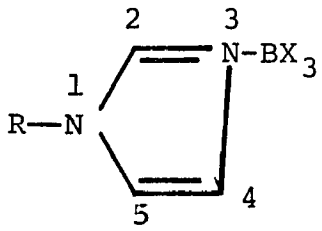

(II)

Unfortunately, the BF_3-N-substituted imidazoles were unstable in the gas phase, dissociating into the acid and base components. This degradation was also observed in the mass spectrometer, where the molecular ion peak of the adduct was not observed but strong peaks corresponding to BF_3 and the N-substituted imidazoles were obtained.

The two highest occupied molecular orbitals in the imidazole ring are π orbitals, the lower energy of the two (IP_2) having a nodal plane through position 2, and the higher energy orbital (IP_1) having a node perpendicular to it.[50] Presumably the former contains more nitrogen character and is analogous to the b_1^* orbital of pyridine, while

---

*Its symmetry is lower but for ease of comparison to the corresponding pyridine we will retain the name.

the latter contains less nitrogen character and is analogous to the a_2 orbital of pyridine.* The nitrogen lone pair orbital is close in energy to the former (IP_2), and it is not separated from IP_2 in the pes of imidazole.[50] Table 33 lists the values of N-substituted imidazoles with a variety of alkyl groups. The decrease in ionization energies is steeper for IP_2 than IP_1 as the substituents become more electron donating, consistent with the fact that IP_1 has a nodal plane near the nitrogens and IP_2 is from an orbital with large nitrogen character (greater substituent interaction with this π orbital).

The N-substituted imidazole-borane complexes show four ionization bands (see Table 34). The first IP is assigned to an ionization from a BH_3 group orbital. IP_2 and IP_3 are assigned to ionizations from π orbitals, the former with very little nitrogen character (similar to $a_2(\pi)$ of pyridine) and the latter with a large nitrogen contribution (similar to $b_1(\pi)$ of pyridine). The fourth ionization band is assigned to the donor lone pair. The pattern of these spectra are similar to BH_3·ethylpyridine (where IP_4 is observed). Energies of stabilizations upon complexation can also be calculated (see Table 35). IP_2, IP_3, and IP_4 in the complex correspond to IP_1, IP_2, and IP_2, respectively in the N-substituted imidazoles.

---

*See Figure 7 for the two highest π molecular orbitals on next page.

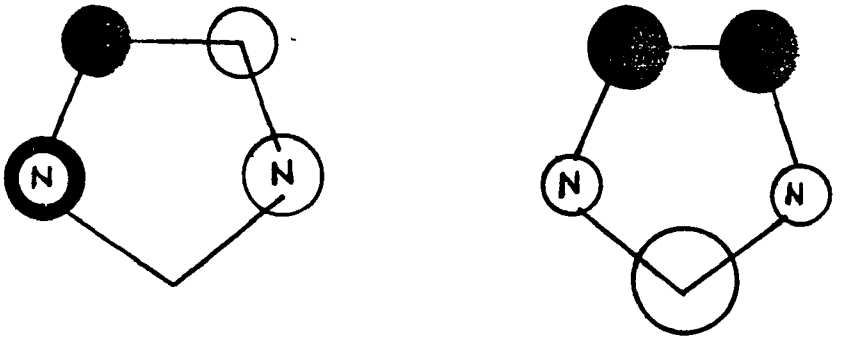

Figure 7. Two highest occupied π molecular orbitals of imidazole.

Table 33: Vertical Ionization Energies of N-Substituted Imidazoles[a]

Compound	IP_1[b]	IP_2[c]
Imidazole	9.03	10.37
N-methylimidazole	8.78	9.95
N-ethylimidazole	8.67	9.85
N-propylimidazole	8.60	9.75

[a] In eV. [b] π orbital with nodal plane perpendicular to the one in IP_2. [c] π orbital with nodal plane through carbon 2.

Table 34: Vertical Ionization Energies of Borane-N-Substituted Imidazoles[a]

Complex	IP_1[b]	IP_2[c]	IP_3[d]	IP_4[e]
BH_3·methylimidazole	9.25	9.80	11.61	12.3
BH_3·ethylimidazole	9.2	9.72	11.45	12.12
BH_3·propylimidazole	9.16	9.75	11.39	12.66

[a] In eV. [b] Borane group orbitals. [c] π orbital that is similar to IP_1 (π) of the corresponding base (see table 33). [d] π orbital that is similar to IP_2 (π) of the corresponding base (see table 33). [e] Donor-acceptor lone pair.

Table 35: Energies of Stabilization Upon Complexation[a]

Complex	Δa_2[b]	Δb_1[c]	Δa_1[d]
BH_3·methylimidazole	1.02	1.65	2.35
BH_3·ethylimidazole	1.05	1.60	2.27
BH_3·propylimidazole	1.15	1.64	2.91

[a]In eV. $\Delta = IP_{COMPLEX} - IP_{BASE}$. [b]$\pi$ orbital that is similar to a_2 of pyridine. [c]π orbital with large contributions from nitrogens. This orbital is similar to b_1 (π) of pyridine. [d]Assigned to donor-acceptor bond.

Discussion

The results of this study indicate that there is no significant interaction between the π systems in the N-substituted imidazoles and the π component of the BH_3 group orbitals. The lack of any observed splitting of the e orbitals (IP_1) suggests that the energy of the π component is not perturbed by the ring any more than the other (σ) component. Comparisons of the corresponding substituted pyridine and imidazole adducts (see Tables 25 and 34) indicate that the e set of BH_3 is at a higher energy in the imidazole adducts. This suggests that imidazoles place more charge at the BH_3 group than pyridines leading to a greater destabilization of BH_3 group orbitals (and smaller IP's). This ordering is consistent with the greater pK_a values found for imidazoles.

By and large the π orbital stabilization energies are constant for the different N-alkyl imidazoles. This observation was also observed for the $4\text{-}RC_5H_4N\cdot BH_3$ complexes (see Table 24). In general, the Δa_2 and Δb_1 magnitudes are larger in the BH_3·N-substituted imidazole adducts than for the BH_3·4-substituted pyridines. This suggests that there is a greater charge depletion from the imidazoles than pyridine upon borane formation, consistent with the observations on the corresponding BH_3 group ionization energies. The ratio $\Delta b_1/\Delta a_2$ in BH_3·

picoline is 1.6 and for BH_3·N-methylimidazole the ratio is also 1.6. The corresponding analysis with ethyl as the substituent results in similar ratios (~ 1.6) for BH_3·N-ethylimidazole and BH_3·N-ethylpyridine. These similar ratios suggest that the two π orbitals found in imidazole at lower symmetry are very similar in character to the more highly symmetric pyridine π orbitals. We had expected a smaller difference in energy of stabilization between the two π orbitals of N-alkylsubstituted imidazoles.

Experimental

N-substituted imidazoles (where substituent = CH_3, C_2H_5, and N-C_3H_7) were purchased from Chemical Dynamics Corporation and were used without further purification. The dimethyl sulfide-borane complex was obtained from Aldrich Chemical Company.

All elemental analyses were performed by Schwarzkopf Microanalytical Labs (see Table 36).

Typical Preparation of BH_3·N-methylimidazole

An excess of dimethyl sulfide-borane was added to a solution of N-methylimidazole in methylene chloride. The reaction warmed quickly upon mixing. The solvent, excess dimethyl sulfide-borane, and dimethyl sulfide were removed under vacuum leaving the product behind. The product gave the correct molecular ion peak and elemental analysis.

Table 36: Elemental Analysis for BH_3·N-Substituted Imidazoles

	Carbon		Hydrogen	
	Calcd.	Found	Calcd.	Found
BH_3·Methylimidazole	50.97	51.06	9.45	9.54
BH_3·Ethylimidazole	54.61	54.60	10.08	10.15
BH_3·Propylimidazole	58.12	58.09	10.57	10.59

APPENDIX I

Background

T. P. Fehlner, J. K. Kochi and coworkers have measured[51] the photoelectron spectra of some heavy group IV alkyls and alkyl hydrides (see Table 37). They pointed out that these ionization potentials serve primarily as a body of information useful in investigating trends in reactivity for processes involving electron transfer. The pes also provide a pleasing example of the simplicity with which the language of molecular orbital theory can be used to explain trends in the energies and nature of the radical cation states of a series of chemically related molecules. For example, the pes for the series $(C_2H_5)_xGeH_{4-x}$ for x = 1 - 4 show that the number of bands and the relative areas of these bands are in accord with predictions of group theory. They also observed a smooth decrease in ionization potential with increasing number of ethyl groups for both the Ge-C and Ge-H bands.

A. F. Orchard, D. W. Turner, J. P. Maier et al.[52] reported that the photoelectron spectra of tetraalkyllead consisted of two broad bands. The lower energy band could be resolved into three bands which had been assigned to ionization from the $3t_2$ orbital derived principally from the σ_{M-C} bonding orbitals. The structure of this band was also explained in terms of Jahn-Teller splitting of the $^2T_2$ molecular ion state.

However, Fehlner and Kochi[51] only discussed the qualitative aspects of the metal-ligand band. We aim to provide a quantitative relationship between Taft σ* values and ionization energies. The following is taken from a note to J. Org. Chem., prepared by Prof. J. K. Kochi.

Table 37: Lowest Ionization Potentials (eV) of Group IV Alkyl Hydrides[a]

Compound	Band 1	Band 2	Band 3
$(C_2H_5)_4Si$	9.8		
$(C_2H_5)_4Ge$	9.4		
$(C_2H_5)_4Sn$	9.0		
$(C_2H_5)_3SiH$	9.9	10.7	
$(i\text{-}C_3H_7)_3SiH$	9.5	10.4	
$(C_2H_5)_3GeH$	9.6	10.5	
$(CH_3)_3SnH$	9.9	10.6	
$(C_2H_5)_3SnH$	9.1	10.0	
$(i\text{-}C_3H_7)_3SnH$	8.6	9.7	
$(n\text{-}C_4H_9)_3SnH$	8.8	9.8	
$(C_2H_5)_2GeH_2$	9.8	10.5	11.2
$(C_2H_5)GeH_3$	10.4	11.6	

[a]Reference 51.

ORGANOMETALS AS ELECTRON DONORS. Effects of Alkyl Groups on the Ionization Potentials of Tetraalkyltin Compounds in the Correlation with Taft σ* Values.

C. L. Wong, K. Mochida, A. Gin, M. Weiner and J. K. Kochi

Departments of Chemistry, Indiana University, Bloomington, Indiana 47401 and The City College of the City University of New York, New York, New York 10031.

Results and Discussion

Organometals, particularly those with alkyl groups as ligands, are excellent electron donors. As electron-rich species they are subject to cleavage by various organic electrophiles including acids, alkyl halides, carbonyl and nitro compounds as well as metal complexes.[53] Since alkylmetals have rather low ionization potentials, electron transfer mechanisms are also possible in which the rate is limited by the ability of the organometal to transfer an electron to an electrophile acting as an electron acceptor. In order to delineate the energetics of such processes, it would be desirable to evaluate

quantitatively the effects of alkyl ligands on the ionization potentials of organometals such as tetraalkyltin compounds, i.e.,

$$R_4Sn \xrightarrow{IP} R_4Sn.^+ + e^- \qquad (7)$$

where R represents the same or different saturated alkyl groups.

The uv photoelectron spectrum (pes) of the parent member of the series, tetramethyltin, shows two well-defined, but broad bands, $\underline{\underline{A}}$ and $\underline{\underline{B}}$, centered at 9.65 and 13.4 eV, respectively, with a shoulder at 14.8 eV.[54] The lowest energy band $\underline{\underline{A}}$, which is of principal concern to us, is associated with ionization from the Sn-C σ-bonding orbital.[52,54,55] Semiempirical calculations for tetramethyltin with tetrahedral (T_d) symmetry are in agreement with a highest occupied molecular orbital (HOMO) which is triply degenerate ($3t_3$).[56,54,56]

The lowest vertical ionization potentials of three series of homologous tetraalkyltin compounds, viz., R_4Sn, $RSnMe_3$ and R_2SnMe_2, are listed in Table 38.[57] For the symmetrical tetraalkyltins, R_4Sn, the values of the first vertical ionization potentials are more or less linearly related to the sums of the Taft polar substituent parameters (σ*) of the alkyl groups,[58] as shown by the

Table 38: Photoelectron Spectra of Tetraalkyltin Compounds

	SnR_4	Σ σ*	IP_1 (eV)			$\overline{IP}$ (eV)
1	Me	0	9.7			9.7
2	Et	.40	8.93			8.93
3	n-Pr	.46	8.82			8.82
4	i-Pr	.76	8.46			8.46
5	n-Bu	.52	8.76			8.76
6	i-Bu	.50	8.68			8.68
7	s-Bu	.84	8.45			8.45
8	neo-Pentyl	.66	8.67			8.67
	Me_2SnR_2	Σ σ*	IP_1	IP_2	IP_3	$\overline{IP}$ (eV)
9	Et[a]	.20	9.01	9.28	0.64	9.31
10	n-Pr	.23	8.8	9.2	9.5	9.17
11	i-Pr	.38	8.56	8.99	9.55	9.03
12	n-Bu	.26	8.8	9.2	9.5	9.17
13	t-Bu	.6	8.22	8.74	9.47	8.81
	Me_3SnR	Σ σ*	IP_1	IP_2		$\overline{IP}$ (eV)
14	Et[a]	.10	9.1	9.5[b]		9.37
15	i-Pr	.19	8.9	9.45 9.76		9.37

	Me_3SnR	$\Sigma\ \sigma^*$	IP_1	IP_2	$\overline{IP}$ (eV)
16	n-Bu	.13	9.0	9.49[b]	9.37
17	i-Bu	.125	9.05	9.50[b]	9.35
18	t-Bu	.30	8.50	9.62[b]	9.24
19	Et_3MeSn	.30	8.95	9.3	9.07

[a]Taken from reference 57. [b]Not completely resolved.

straight line drawn through these points in Figure 8. However, considerable scatter is encountered when the same plots of the data are attempted for the two series of the methyl-substituted analogs, viz., $RSnMe_3$ and $RSnMe_2$. In these unsymmetrical tetraalkyltins, symmetry considerations predict the band $\underline{\underline{A}}$ of R_4Sn to be split into additional bands.[59,*] In particular, for the monosubstituted derivatives $RSnMe_3$ with C_3 symmetry, band $\underline{\underline{A}}$ would be split into an a_1 and doubly degenerate e set, whereas for the disubstituted analogs R_2SnMe_2 with C_{2v} symmetry, it would be split into a b_1, a and b_2 set, as the correlation diagram in Figure 9 illustrates for the complete series of five methylethyltin compounds. Indeed, the experimental spectrum for Me_3SnBu^t shown in Appendix II shows a doublet splitting with the expected 1:2 intensity ratio for this low energy band. It is noteworthy that a similar splitting pattern is observed with Et_3SnMe but in a reversed 2:1 intensity ratio. Furthermore, the pes spectrum of $Me_2SnBu^t_2$ in Appendix II shows two distinct splittings associated with the three energy levels predicted by this simple formulation.[51]

If we take cognizance of these splittings of the HOMO of tetramethyltin, as they are induced by methyl substitutions, it would appear that the Taft σ* parameter should correlate better with the weighted (center

---

*Ignoring Jahn-Teller distortion of the $^2T_2$ state of the parent molecule-ion.

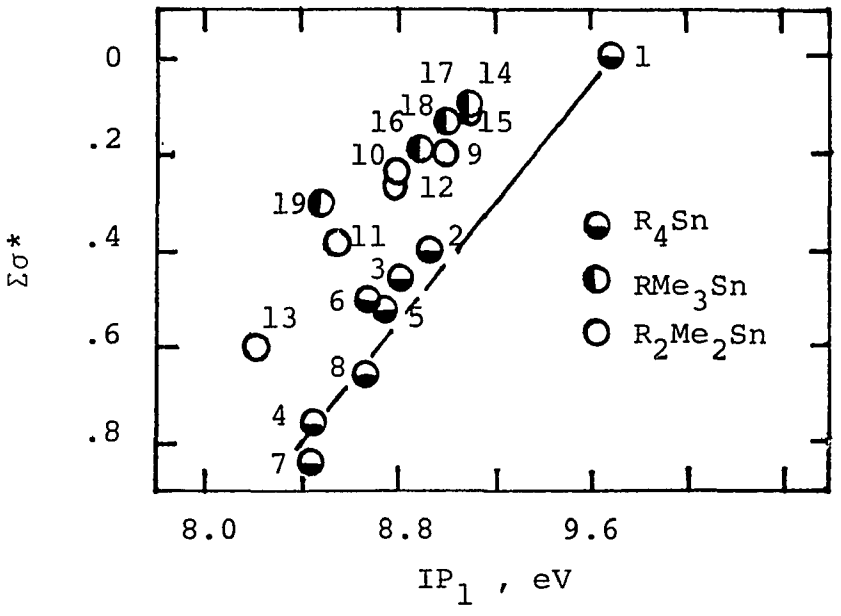

Figure 8. Relationship between the first vertical ionization potentials of a homologous series of symmetrical R_4Sn ◒, unsymmetrical $RSnMe_3$ ◐ and R_2SnMe_2 O tetraalkyltin compounds and the sum of the Taft polar substituent parameters $\Sigma\sigma^*$. Numbers refer to the listing of compounds in Table 38. Straight line drawn through R_4Sn compounds only (see text).

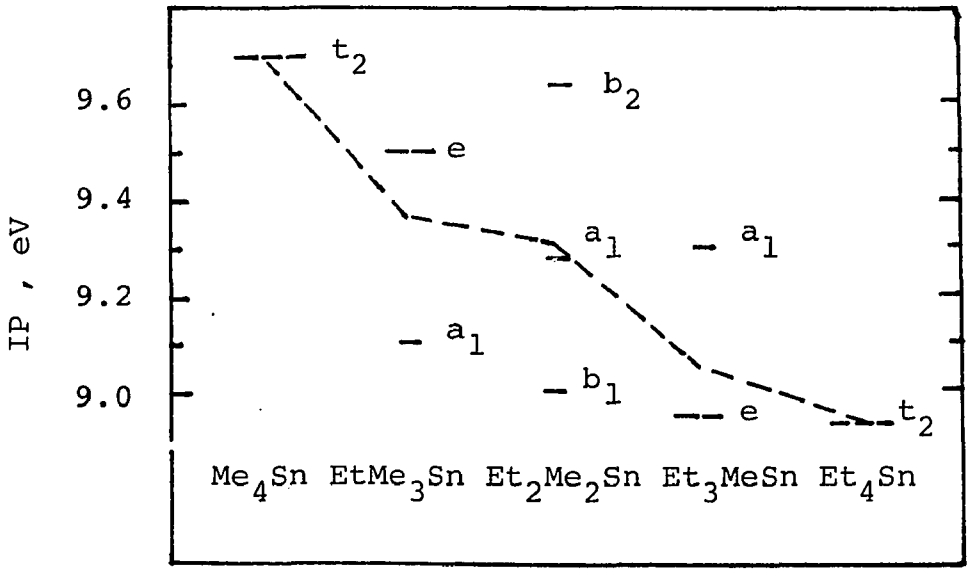

Figure 9. Correlation diagrams for the triply degenerate t molecular orbital of tetramethyltin as a result of successive substitution of ethyl for methyl ligands.

of gravity) average of all the vertical ionization potentials included in the first band $\underline{\underline{A}}$. Such an averaging procedure is tantamount to choosing a single (imaginary) ionization potential, $\overline{IP}$, to represent each tetraalkyltin, irrespective of its substitution pattern. The dashed line in Figure 9 is drawn through $\overline{IP}$ for each $Me_{4-n}Et_nSn$. Indeed, Figure 10 shows that the averaged ionization potentials for all the various tetraalkyltins included in Figure 8 are now well correlated with the Taft σ^* values by a single line.

In the series of monosubstituted tetraalkyltins, $RSnMe_3$, the energy difference Δ between the e and a_1 molecular orbitals (see Figure 11) reflects the perturbation of the triply degenerate t_2 levels in tetramethyltin as a result of successive methyl substitutions at a single methyl ligand [i.e., R = CH_3, CH_3CH_2, $CH_3CH_2CH_2$, $(CH_3)_2CH$, $(CH_3)_3C$, etc.].* As such it is reasonable to expect the magnitude of this splitting to be reflected in the Taft σ^* value for R, as shown in Figure 11. It is noteworthy that the linear correlation passes through the origin, i.e.,

$$\Delta = 3.7\sigma^* \text{ eV} \qquad (8)$$

in accord with this simple formulation. Thus for a series

---

*The splitting is actually 2/3 Δ.

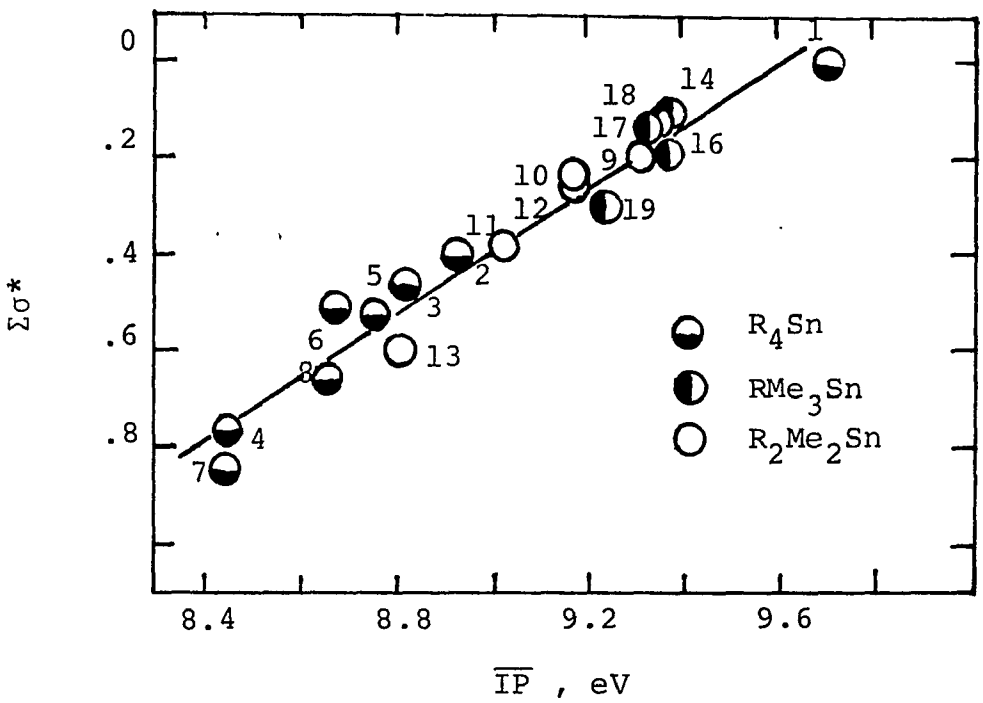

Figure 10. Linear correlation of the weighted average ionization potentials $\overline{IP}$ and Taft $\Sigma\sigma^*$ parameters for the same tetraalkyltin compounds listed in Figure 8.

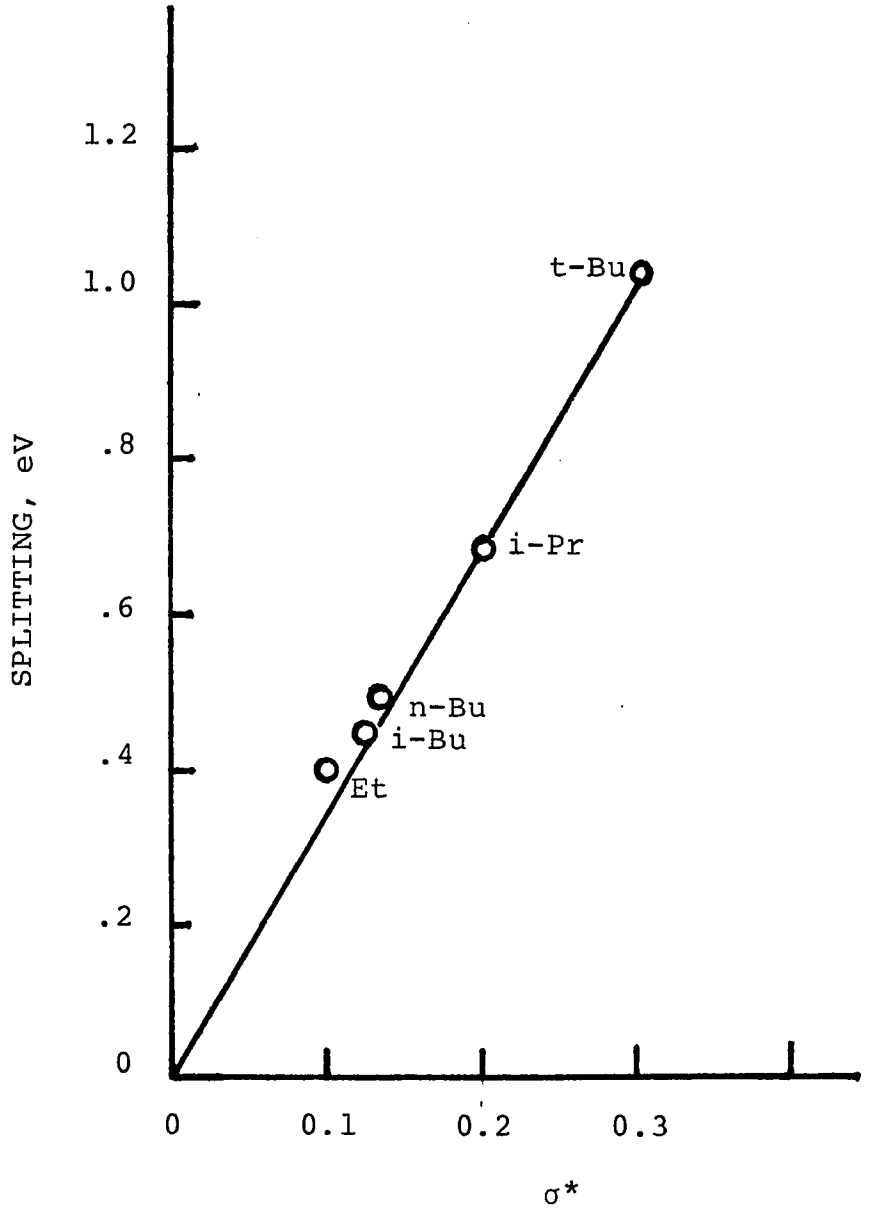

Figure 11. Electronic effects of alkyl ligands (R) measured by Taft σ^* values on the splitting of the e and a_1 levels in a series of alkyltrimethyltin (RSnMe) compounds. Note the extrapolation through the origin.

of unsymmetrical tetraalkyltins $RSnMe_3$, the first vertical ionization potential from $HOMO_1$* can be simply related to the ionization potential (IP_1 = 9.70 eV) of tetramethyltin from its Taft σ* value, i.e.,

$$IP_1(RSnMe_3) = 9.70 - 4.3\ \sigma^* \qquad (9)$$

The experimental and calculated ionization potentials for a series of $RSnMe_3$ are compared in Table 39.

---

*Assuming Koopmans' theorem.

Table 39: Experimental and Calculated Values of the First Vertical Ionization Potentials of Alkyltrimethyltin Compounds

$RSnMe_3$ R	IP_1(expt.) (eV)	IP_1(calcd.)[a] (eV)
Me	9.70	9.70
Et	9.1	9.27
n-Bu	9.0	9.14
i-Bu	9.05	9.16
i-Pr	8.9	8.88
t-Bu	8.5	8.41

[a]Calculated from equation 9.

Experimental Section

Materials. Tin tetrachloride, obtained as a generous sample from M and T Chemical Co. Inc., was used in all the syntheses of tetraalkyltin compounds. The symmetrical R_4Sn were prepared by the exhaustive alkylation of $SnCl_4$ with the appropriate Grignard reagent.[64] A typical example is: 70 g (0.27 mol) stannic chloride was added dropwise to 1.5 mol EtMgBr in ether under a nitrogen atmosphere. The reaction was refluxed for 4 hrs after the addition was completed, and hydrolyzed with dilute (0.1 N) aqueous HCl. After repeated extractions with ether, the combined ethereal layer was finally washed with saturated $NaHCO_3$ and dried over $CaCl_2$. Distillation following the removal of solvent afforded Et_4Sn, bp. 84°C/11 mm.[60] Others were R_4Sn (bp.): Me_4Sn (78°C/758 mm),[61] n-Pr_4Sn (79°C/2 mm),[60] i-Pr_4Sn (102°C/30 mm),[60] n-Bu_4Sn (92°C/1 mm),[60] i-Bu_4Sn (101°C/1.5 mm),[60] s-Bu_4Sn (108°C/0.8 mm),[61] and neo-$Pent_4Sn$ (mp. 124°C after three recrystallizations from n-hexane).[62]

The unsymmetrical tetraalkyltin compounds, $RSnMe_3$ and R_2SnMe_2, were prepared by a similar procedure starting with Me_3SnCl and Me_2SnCl_2, respectively. Trimethyltin chloride was prepared either from Me_4Sn by HCl cleavage or by syn proportionation with a stoichiometric amount

of $SnCl_4$. Dimethyltin dichloride was prepared from Me_4Sn and $SnCl_4$ at 130°C for 4 hrs. Triethyltin chloride was prepared from Et_4Sn and acetyl chloride in the presence of aluminum chloride. $RSnMe_3$ (bp.): $EtSnMe_3$ (105°C/760 mm),[60] n-$PrSnMe_3$ (131°C/760 mm),[63] i-$PrSnMe_3$ (123°C/120 mm),[64] n-$BuSnMe_3$ (150°C/750 mm),[60] t-$BuSnMe_3$ (56°C/36 mm).[65] R_2SnMe_2 (bp.): Et_2SnMe_2 (65°C/50 mm),[64] n-Pr_2SnMe_2 (74°C/30 mm),[64] i-Pr_2SnMe_2 (66°C/30 mm),[60] n-Bu_2SnMe_2 (70°C/4 mm),[60] t-Bu_2SnMe_2 (75°C/30 mm).[60,66] i-Bu_2SnEt_2[60] was prepared from i-BuMgCl and Et_2SnCl_2 (from Et_4Sn and $SnCl_4$) (bp. 124°C/13 mm).

All the spectra were obtained with a Perkin-Elmer PS-18 photoelectron spectrometer using the He(I) resonance line at 21.22 eV. The spectra were calibrated with Ar lines at 15.759 and 15.937 eV. In most cases the vapor pressures of the tetraalkyltin were sufficient to carry out the spectral studies at ambient temperature.

Acknowledgment. We wish to thank the National Science Foundation for financial support [Grant no. CHE74-21010 to J. K. Kochi] of this work.

APPENDIX II

$Cr(CO)_5$pyridine

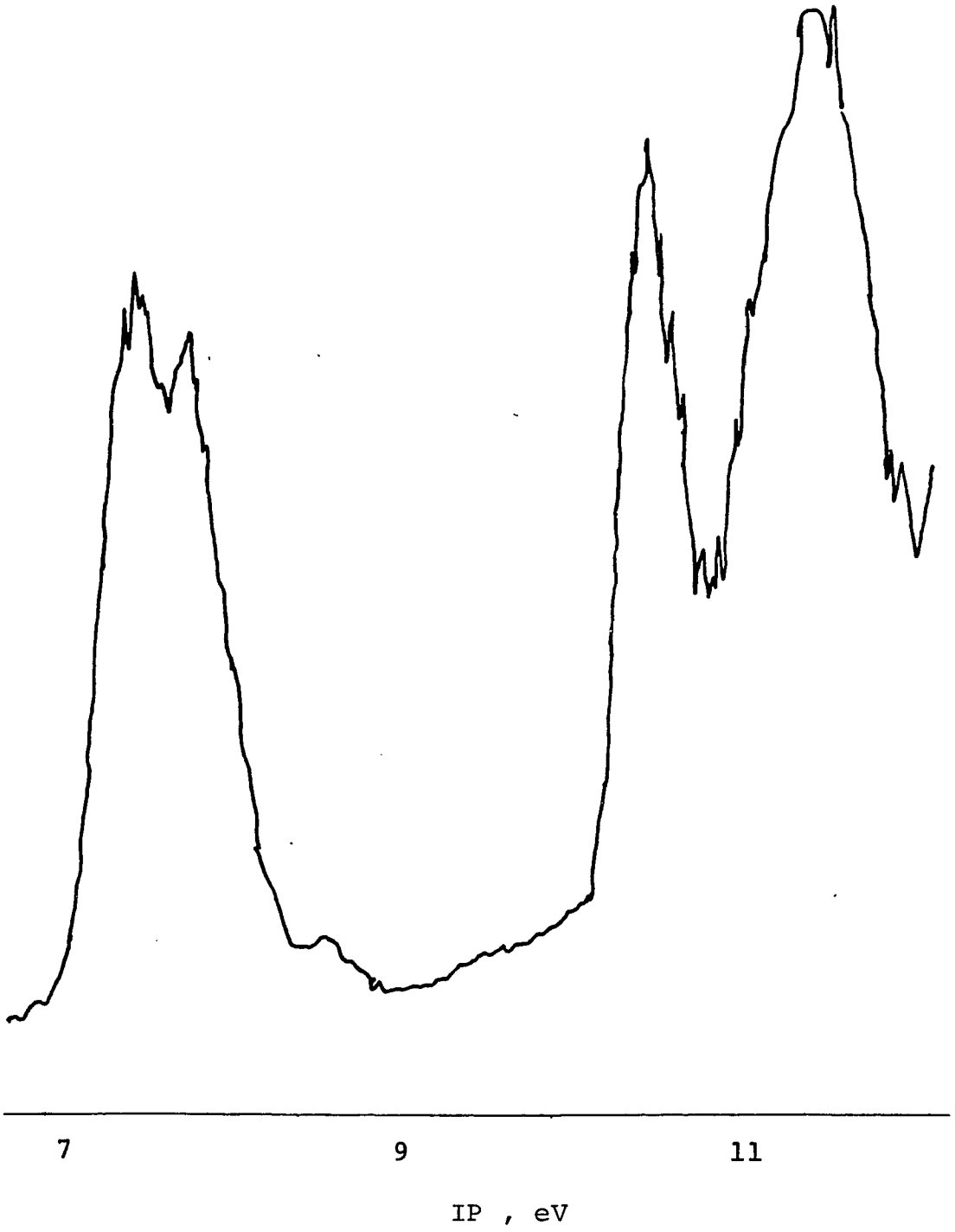

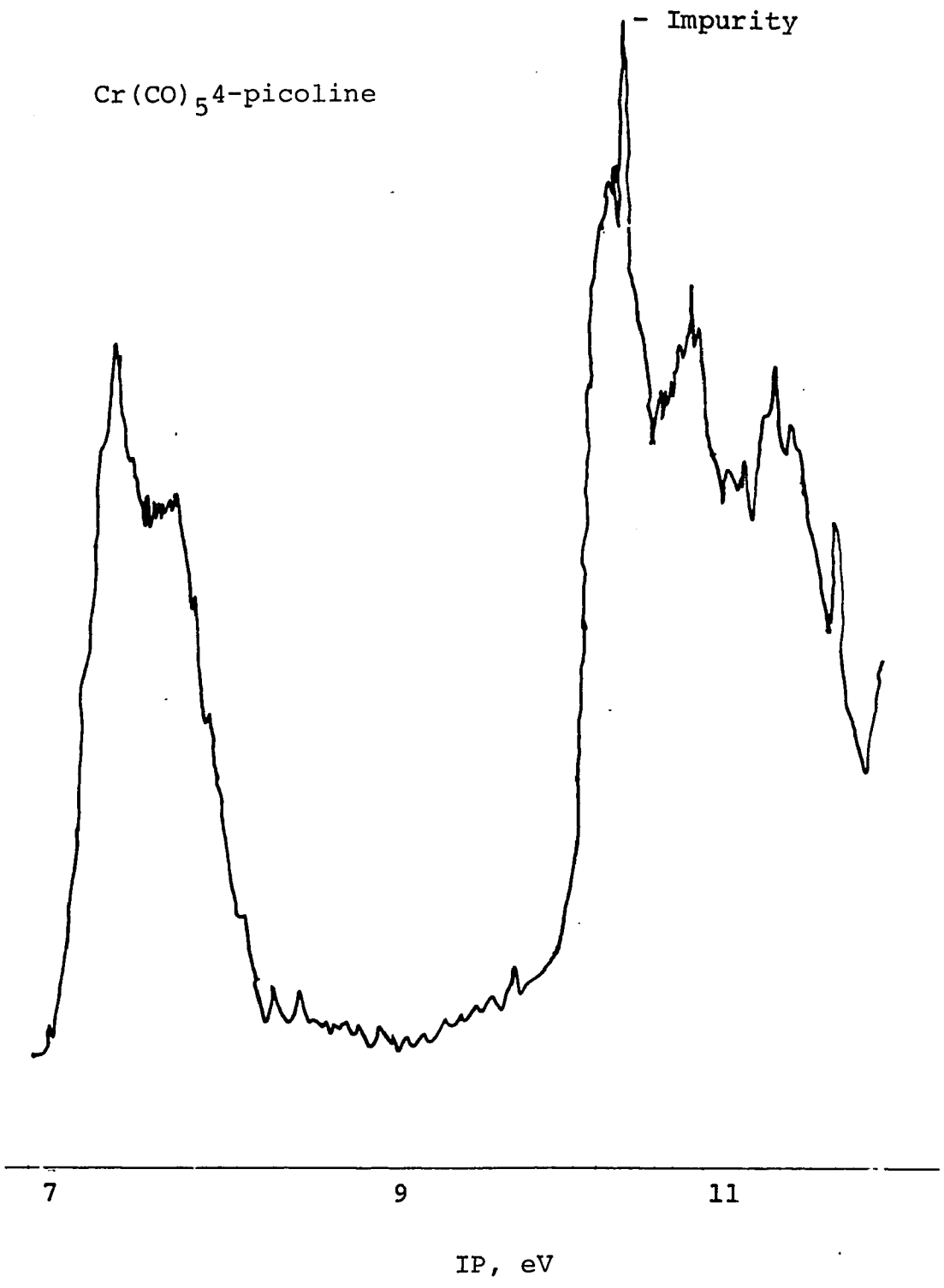
Impurity
Cr(CO)5 4-picoline
7
9
11
IP, eV

Me_3SnBu^t

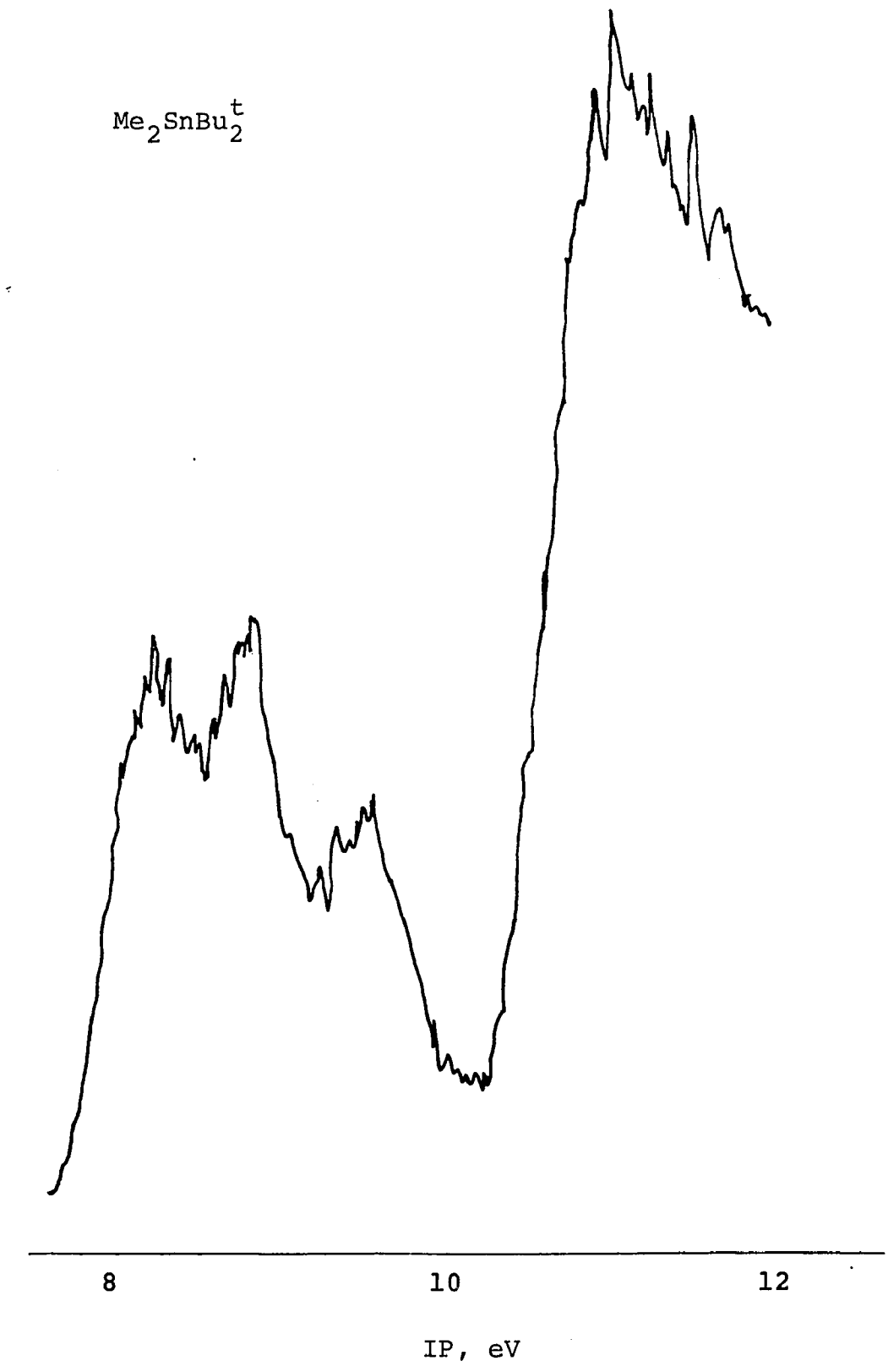
$Me_2SnBu^t_2$
8
10
12
IP, eV

BH_3·ethylpyridine

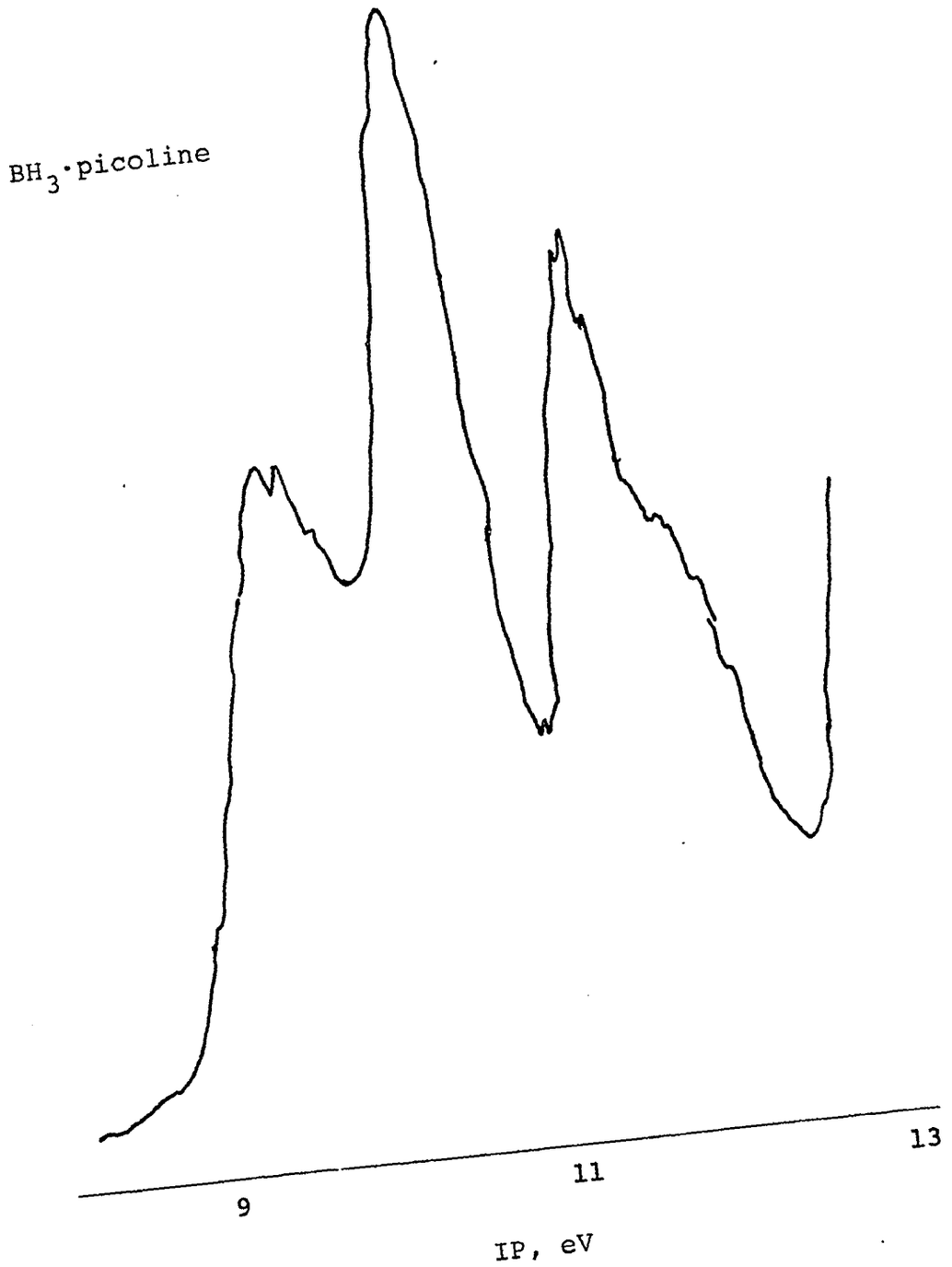
BH_3·picoline
9
11
13
IP, eV

BF_3·picoline

BIBLIOGRAPHY

1. Al-Joboury, M. I. and Turner, D. W., J. Chem. Soc., 1963, 5141.

2. Al-Joboury, M. I. and Turner, D. W., J. Chem. Phys., 1962, 37, 3007.

3. Vilesov, F. I.; Kurbatov, B. L. and Terenin, A. N., Dokl. Akad. Nauk S.S.S.R., 1961, 138, 1329.

4a. Baker, A. D., Accts. Chem. Res., 1970, 3, 17; b. Worley, S. D., Chem. Revs., 1971, 71, 295; c. Wittel, K. and McGlynn, S. P., Chem. Revs., 1977, 77, 745.

5a. Eland, J. H. D., Photoelectron Spectroscopy, Wiley, New York, N.Y., 1974; b. Rabalais, J. W., Principles of Photoelectron Spectroscopy, J. Wiley and Sons, New York, N.Y., 1977; c. Turner, D. W.; Baker, C.; Baker, A. D. and Brundle, C. R., Molecular Photoelectron Spectroscopy, Wiley, New York, N.Y., 1970; d. Carlson, T. A., Photoelectron and Auger Spectroscopy, Plenum Press, New York, N.Y., 1977.

6. Koopmans, T., Physica, 1933, 1, 104.

7. Higginson, B. R.; Lloyd, D. R.; Connor, J. A.; Hillier, I. H.; J. Chem. Soc. Faraday Trans. II, 1974, 70, 14, 1418.

8. Daaman, H.; Oskam, A., Inorg. Chim. Acta, 1978, 26, 81.

9. Ramsey, B.; Walker, F., J. Am. Chem. Soc., 1974, 96, 3314.

10. Weiner, M. A. and Lattman, M., Inorg. Chem., 1978, 17, 1084.

11. Yarbrough, L. W. and Hall, M. B., Inorg. Chem., 1978, 17, 2269.

12. Lichtenberger, P. L. and Fenske, R. F., Inorg. Chem., 1976, 15, 2015.

13. Karlsson, L.; Bergmark, T.; Jodrny, R.; Siegbahn, K.; Gronowitz, S. and Maltesson, A., Chemica Scripta, 1974, 6, 214.

14. Heilbronner, E.; Hornung, V.; Pinkerton, F. H. and Thames, S. F., Helv. Chim. Acta, 1972, 55, 289.

15. Bock, H., Pure Appl. Chem., 1975, 44, 343.

16. Connor, J. A.; Jones, E. M. and Mekwen, G. K., J. Organometal. Chem., 1972, 43, 357.

17. Abel, W. W.; Butler, I. S. and Reid, J. G., J. Chem. Soc., 1963, 2068.

18. Miller, J., Angew. Chem. Int. Ed. Engl., 1972, 11, 653.

19. Brehrens, H. and Kohler, J., Z. Anorg. Allgem. Chem., 1959, 300, 51.

20. Strohmeier, W.; Matthias, G. and Hobe, D. V., Z. Naturforsch., 1960, 15b, 813.

21. Higginson, B. R.; Lloyd, D. R.; Burroughs, P.; Gibson, D. M. and Orchard, A. F., J. Chem. Soc. Faraday II, 1973, 69, 1659.

22. Weiner, M. A.; Gin, A. and Lattman, M., Inorg. Chim. Acta, 1977, 24, 235

23. Weiner, M. A. and Lattman, M., Tetrahedron Letters, 1974, 18, 1709.

24. Thesis of Michael Lattman, City University of New York, 1977.

25. Weiner, M. A. and Lattman, M., Inorg. Nucl. Chem. Letters, 1975, 11, 723.

26. Wrighton, M. S.; Abrahamson, H. B. and Morse, D. L., J. Am. Chem. Soc., 1976, 98, 4105.

27. Mester, M. A. M.; Vriends, R. C. J.; Stufkens, D. J. and Vrieze, K., Inorg. Chim. Acta, 1976, 19, 95.

28. Dennenberg, R. J. and Darensbourg, D. J., Inorg. Chem., 1972, 11, 72.

29. Prins, D. A., Rec. Trav. Chim. Pays-Bas, 1957, 76, 58.

30. Lake, R. L., Spectrochim. Acta, 1971, 27A, 1220.

31. Aue, D. H.; Webb, H. M. and Bowers, M. T., J. Am. Chem. Soc., 1976, 98, 311.

32. Aue, D. H.; Webb, H. M. and Bowers, M. T., J. Am. Chem. Soc., 1975, 97, 4138.

33. Gates, P. N.; Mehauchand, E. J. and Mooney, E. F., Spectrochim Acta, 1965, 21, 1445.

34. Barber, M.; Conner, J. A.; Guest, M. F.; Hillier, I. H.; Schwartz, M. and Stacey, M., J. Chem. Soc. Faraday Trans. 2, 1973, 551.

35. Bock, H., Pure Appl. Chem., 1975, 44, 343.

36. Lloyd, D. R. and Lynaugh, N., J. Chem. Soc., Faraday Trans. 2, 1972, 68, 947.

37. For example, see Hsieh, Y. N.; Rubenacker, G. V.; Cheng, C. P. and Brown, T. L., J. Am. Chem. Soc., 1977, 99, 1384.

38. Celius, U.; Roos, B. and Siegbahn, P., Chem. Phys. Lett., 1970, 4, 471.

39. Young, D. E.; McAcran, G. E. and Shore, S. G., J. Am. Chem. Soc., 1966, 88, 4390.

40a. (a) Coyle, T. D. and Stone, F. G. A., Progress in Boron Chemistry, vol. 1, Steinberg, H. and McClosky, A. L., Ed., Macmillan, New York, 1964; (b) Shriver, D. G. and Swanson, B., Inorg. Chem., 1971, 10, 1354; (c) Brown, D. G., Drago, R. S. and Bolles, T. F., J. Am. Chem. Soc., 1968, 90, 5206.

41. Cassoux, P.; Kuczkowski, R. L. and Seragini, A., Inorg. Chem., 1977, 16, 3005.

42. Brown, D. G.; Drago, R. S. and Bolles, T. F., J. Am. Chem. Soc., 1968, 90, 3005.

43. Bax, C. M.; Katritzky, A. R. and Sutton, L. E., J. Am. Chem. Soc., 1943, 65, 1838.

44. Shriver, D. F. and Swanson, B., Inorg. Chem., 1971, 10, 1354.

45. Vander Meulen, P. A. and Heller, H., J. Am. Chem. Soc., 1932, 54, 4404.

46. Boudakin, M., United States Patent Office, 3,703,521 Nov. 21, 1972

47. Walker, T. E. H. and Horsley, J. A., Mol. Phys., 1971, 21, 939.

48. Dewar, M. J. S. and Rzepa, H. S., J. Am. Chem. Soc., 1978, 100, 58.

49. Jaffe, H. H. and Del Bene, J., J. Chem. Phys., 1968, 48, 1807.

50. Craddock, S.; Findlay, R. H. and Palmer, M. H., Tetrahedron, 1973, 29, 2173.

51. Beltram, G.; Fehlner, T. P.; Mochida, K. and Kochi, J. K., J. Electron Spectrosc., submitted for publication.

52. Evans, S.; Green, J. C.; Joachin, P. J.; Orchard, A. F.; Turner, D. W. and Maier, J. P., J. Chem. Soc. Faraday Trans. II, 1974, 68, 905.

53. Kochi, J. K., Organometallic Mechanisms and Catalysis, Academic Press, New York, 1978, 445.

54. Jonas, A. E.; Schweitzer, G. K.; Grimm, F. A. and Carlson, T. A., J. Electron Spectrosc., 1972, 1, 29.

55. Boschi, R.; Lappert, M. F.; Pedley, J. B.; Schmidt, W. and Wilkins, B. T., J. Organometal. Chem., 1973, 50, 69.

56. Compare also Schmidt, W. and Wilkins, B. T., Angew. Chem. Int. Ed., Engl., 1972, 11, 221.

57. For the early work on pes of various organotin compounds, see Hosomi, A. and Traylor, T. G., J. Am. Chem. Soc., 1975, 97, 3682.

58. Taft, R. W. Jr., Steric Effects in Organic Chemistry, Newman, M. S., ed., J. Wiley & Sons, Inc., New York, N.Y., 1956, 586.

59. Burdett, J. K., Structure Bonding, 1976, 31, 67.

60. Ingham, R. K.; Rosenberg, S. D. and Gilman, H., Chem. Revs., 1960, 60, 459, and references cited therein.

61. Newman, W. P.; Schneider, B. and Sommer, R., Ann. 1966, 692, 1.

62. Zimmer, H.; Hechenbleikner, I.; Homberg, O. A. and Danzik, M., J. Org. Chem., 1964, 29, 2632.

63. Pollard, F. H.; Nickless, G. and Dolan, D. N., Chem. Ind., 1965, 1027.

64. Boué, S.; Gielen, M. and Nasielski, J., J. Organometal. Chem., 1967, 9, 443.

65. Putnam, R. C. and Pu, H., J. Gas Chromatography, 1965, 3, 160.

66. Kandil, S. A. and Allred, A. L., J. Chem. Soc. A, 1970, 2987.